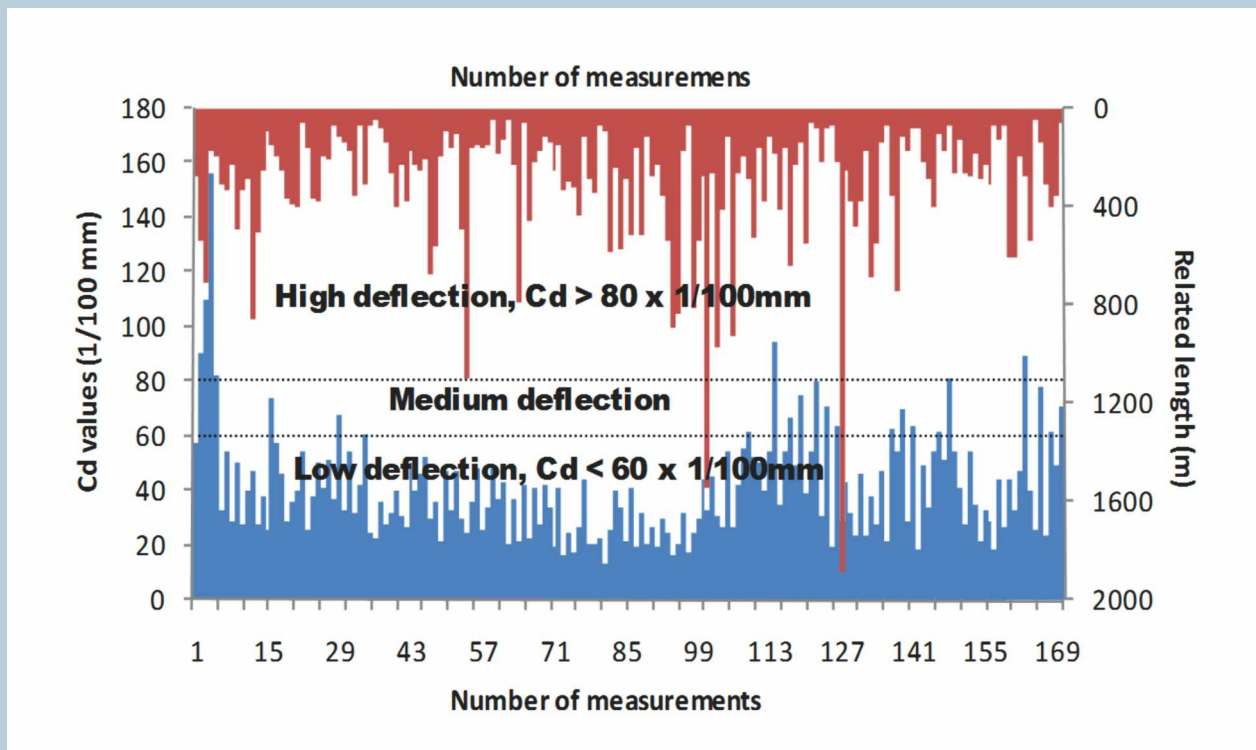


Geomaterials



Journal Editorial Board

ISSN 2161-7538 (Print) ISSN 2161-7546 (Online)

<http://www.scirp.org/journal/gm>

Editor-in-Chief

Prof. Zhijian Peng China University of Geosciences, China

Editorial Board

Dr. Kerim Aydiner Karadeniz Technical University, Turkey
Prof. Khairun Azizi University Teknologi PETRONAS, Malaysia
Dr. Rituparna Bose The City University of New York, USA
Dr. Karra Ram Chandar National Institute of Technology Karnataka, India
Prof. Kaan Erarslan Dumlupinar University, Turkey
Prof. B. M. Girish East Point College of Engineering and Technology, India
Prof. M. Jayachandran Central Electrochemical Research Institute, India
Prof. Yilmaz Ozelik Hacettepe University, Turkey
Dr. Partha Patra Columbia University, USA
Prof. Gehad Mohamed Saleh Nuclear Materials Authority (NMA), Egypt
Prof. Cem Şensöğüt Dumlupinar University, Turkey
Prof. T. N. Singh IIT Bombay, India
Prof. Vladimir E. Vigdergauz Russian Academy of Sciences, Russia
Prof. Huaming Yang Central South University, China
Prof. Kun Zhao China University of Petroleum, China
Prof. Liancun Zheng University of Science and Technology (Beijing), China

Table of Contents

Volume 5 Number 1

January 2015

Applying Empirical Methods to Assess the Internal Stability of Embankment Dam Cores of Glacial Till

H. Rönnqvist, P. Viklander.....1

Evaluation of the Impact of Truck Overloading on Flexible Compacted Gravel Lateritic Soil's Pavements by FEM with Cast3M[®]

F. Samb, M. Fall, Y. Berthaud, F. Bendboudjema.....19

Field Scale Simulation Study of Miscible Water Alternating CO₂ Injection Process in Fractured Reservoirs

M. A. Karaei, A. Ahmadi, H. Fallah, S. B. Kashkooli, J. T. Bahmanbeglo.....25

Diagnosis Study of the Louga-Ouarack-Ndoyene R31 Regional Road (Senegal)

S. Diop, M. Fall, A. Dione, M. N. Tijani.....34

Geomaterials (GM)

Journal Information

SUBSCRIPTIONS

The *Geomaterials* (Online at Scientific Research Publishing, www.SciRP.org) is published quarterly by Scientific Research Publishing, Inc., USA.

Subscription rates:

Print: \$79 per issue.

To subscribe, please contact Journals Subscriptions Department, E-mail: sub@scirp.org

SERVICES

Advertisements

Advertisement Sales Department, E-mail: service@scirp.org

Reprints (minimum quantity 100 copies)

Reprints Co-ordinator, Scientific Research Publishing, Inc., USA.

E-mail: sub@scirp.org

COPYRIGHT

COPYRIGHT AND REUSE RIGHTS FOR THE FRONT MATTER OF THE JOURNAL:

Copyright © 2015 by Scientific Research Publishing Inc.

This work is licensed under the Creative Commons Attribution International License (CC BY).

<http://creativecommons.org/licenses/by/4.0/>

COPYRIGHT FOR INDIVIDUAL PAPERS OF THE JOURNAL:

Copyright © 2015 by author(s) and Scientific Research Publishing Inc.

REUSE RIGHTS FOR INDIVIDUAL PAPERS:

Note: At SCIRP authors can choose between CC BY and CC BY-NC. Please consult each paper for its reuse rights.

DISCLAIMER OF LIABILITY

Statements and opinions expressed in the articles and communications are those of the individual contributors and not the statements and opinion of Scientific Research Publishing, Inc. We assume no responsibility or liability for any damage or injury to persons or property arising out of the use of any materials, instructions, methods or ideas contained herein. We expressly disclaim any implied warranties of merchantability or fitness for a particular purpose. If expert assistance is required, the services of a competent professional person should be sought.

PRODUCTION INFORMATION

For manuscripts that have been accepted for publication, please contact:

E-mail: gm@scirp.org

Applying Empirical Methods to Assess the Internal Stability of Embankment Dam Cores of Glacial Till

Hans Rönnqvist, Peter Viklander

Department of Civil, Environmental and Natural Resources Engineering, Luleå University of Technology, Luleå, Sweden

Email: hans.ronqvist@ltu.se, peter.viklander@ltu.se

Received 18 October 2014; revised 15 November 2014; accepted 8 December 2014

Copyright © 2015 by authors and Scientific Research Publishing Inc.

This work is licensed under the Creative Commons Attribution International License (CC BY).

<http://creativecommons.org/licenses/by/4.0/>



Open Access

Abstract

This paper presents a database of glacial till gradations that are compiled from laboratory internal stability tests from the literature and from core soils of existing dams, some of which have experienced internal erosion. The potential internal instability of these gradations is assessed using empirical methods. Two approaches of evaluation are used: the Kenney-Lau method, which analyzes the shape of the gradation curve; and the Burenkova method, which uses factors of uniformity of the slope of the gradation. Although they include some uncertainties in terms of soils with fines, these methods, which are primarily developed from laboratory studies of sand and gravels, are used in engineering practice to evaluate widely graded soils that include fines, such as glacial tills. This study evaluates the glacial till gradations of the database using these approaches and discusses their applicability and relative predictive success. This study indicates that both the Kenney-Lau method and the Burenkova method have merit, but a closer analysis indicates that the Kenney-Lau approach has relatively better predictive ability based on the glacial till gradations analyzed in this study.

Keywords

Internal Stability, Internal Erosion, Cores, Glacial Tills, Embankment Dams

1. Introduction

Glacial till, which is a moraine deposit that is formed by glacial action, is commonly used to form impervious cores of embankment dams. When designed and constructed properly, glacial till is highly suitable for dam

cores [1] [2]. However, these cores have a statistically higher frequency of internal erosion incidents than dams with other types of core soils [3] [4]. Typical symptoms of internal erosion include sinkholes and settlements on the crest, increased seepage and cloudy seepage [3] [5]. Internal erosion occurs when soil particles are carried downstream by seepage. ICOLD [6] recognizes four mechanisms of initiation: concentrated leak erosion, backward erosion, contact erosion and suffusion. The overrepresentation of glacial till cores in internal erosion incidents is possibly due to the erodibility of glacial till. One mechanism that may influence internal erosion is suffusion due to internal instability. Suffusion erodes free moving fines inside a soil and can change the geotechnical properties of the soil [6].

Based on engineering practice, Sherard [7] attributed the notably high frequency of sinkhole formations in dams with this type of core to the internal instability of the glacial till. However, few laboratory studies have been performed, and little data are available. Nonetheless, the internal stability of glacial tills has been investigated by Lafleur and Nguyen [8], Wan [9], Moffat *et al.* [10], Hunter *et al.* [11] and Lilja *et al.* [12], who report that instability may indeed occur in glacial tills.

This study compiles a database of 24 gradations of glacial till that includes gradations identified in the literature review of laboratory internal stability tests on glacial tills by Rönnqvist and Viklander [13] (reproduced after [8]-[12]) as well as gradations of glacial till from the cores of existing dams, some of which have experienced internal erosion (reproduced after [14]). This study assesses the potential internal instability of these gradations using empirical methods. Two approaches of evaluation are used: the Kenney-Lau method [15] [16], which analyzes the shape of the gradation curve; and the Burenkova method [17], which uses characteristic values of the slope of the gradation (factors of uniformity). These methods, which are primarily developed from laboratory studies of sand and gravel, are used in engineering practice to analyze widely graded soils that contain fines, such as glacial tills. This may cause some uncertainty. The glacial till gradations of the database are evaluated using these approaches, and their applicability and relative predictive success when they are used to analyze gradations that are different from those that are originally tested are discussed.

2. Glacial Tills

Moraine formations are created by the pulling, crushing, mixing and transport forces generated by the advancement and regression of glaciers. Glacial till, which is collected from moraine deposits, has been widely used as fill for the impervious cores of dams [7]. Till is relatively similar throughout the world; is it typically broadly or widely graded with a mixture of contents that ranges from fines to boulders (Figure 1). In the field of dam engineering, ICOLD [18] defines glacial till as “an unsorted material of glacial origin (...) used as foundations and

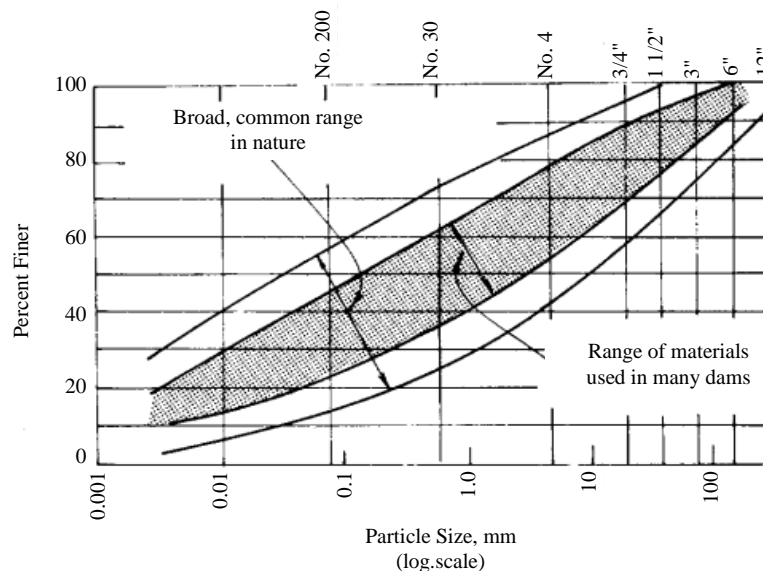


Figure 1. Typical broadly graded glacial soils used as impervious cores in dams (after [21]).

as the impervious zone of earth and rockfill dams”. ICOLD [18] continues by stating that the composition and grain size distribution generally depend on the source rock and the overburden over which the glacier moves; granite, granitic gneiss and similar hard and massive rocks develop tills with a sandy silt matrix, whereas softer sedimentary rocks, such as limestone and shale, develop a clayey matrix. As reported by Milligan [19], softer sedimentary bedrock in Canada generally forms tills with high plasticity fines (as in the Canadian western prairie provinces), whereas harder igneous and metamorphic bedrock forms tills with non-plastic or low plasticity fines (such as in eastern Canada). Examples from other regions include the clayey matrix of British glacial tills [20] and the low-clay and generally non-plastic glacial tills in Scandinavia [1] [2]. North American glacial tills that are used as dam cores are relatively fines-rich with fines contents of 20% to 70%. Scandinavian tills typically contain 15% to 60% fines, and glacial tills in Russian dams are fines-poor with fines contents of 5% to 20% [18]. Fines content is the amount passing the #200 sieve (0.075 mm).

3. Internal Instability and Erosion by Suffusion

A soil that is internally stable has a gradation in which all of the particles contribute to the skeletal structure of the soil. The gradation is illustrated by the particle size distribution of the soil, which shows the relative amount by mass that is contributed by the soil particles. An unstable gradation has an imbalance in the distribution of particles so that the soil is divided into a coarser fraction and a finer fraction; the coarser fraction becomes structural with few highly stressed particle contacts, whereas the finer fraction is non-structural with no effective stress transfer between grains. Thus, in internally unstable soils, the finer fraction comprises moveable and potentially erodible particles.

3.1. Geometrical Requirements for Suffusion

Suffusion is an internal erosion process that is caused by internal instability and involves the “selective erosion of finer particles from the matrix of coarser particles (...) leaving behind a soil skeleton formed by the coarser particles” [6]. For suffusion to occur, the finer fraction of the soil must be less than the available void space in the coarser fraction [22]. A soil that consists predominately of a finer fraction (*i.e.*, a matrix-supported soil) is thus not susceptible to suffusion because the coarser grains are not in grain-to-grain contact but float in the matrix of the finer fraction.

Several opinions on the limit value of the finer fraction for suffusion susceptible soil have been presented in the literature. Wan and Fell [22] argued that the limit is between 22% and 33% and is unlikely to be higher than 40% based on tests on broadly graded samples, while Skempton and Brogan [23] estimated the limit as 35%. Kenney and Lau [15] empirically determined the limit to be 20% based on the lost particles of the unstable widely graded soils that they tested. A widely graded soil is most likely not susceptible to suffusion unless the finer fraction is less than approximately 25% to 35%. According to ICOLD [6], the finer fraction is determined from the inflection point of the gradation; *i.e.*, the change in slope from the initial slope of the coarse fraction to its transition to the finer fraction (**Figure 2(a)**). This transition may be difficult to identify. Applications of this procedure to fines-rich and fines-poor glacial till gradations are shown schematically in **Figure 2(b)**.

3.2. Effects of Suffusion

Although suffusion has been reported to increase the permeability [6], laboratory studies also indicate that suffusion results in clogging with zones of low permeability, increased gradients and pore pressure build-up [8] [24]. Furthermore, Moffat *et al.* [10] found that suffusion occurred as the “episodic migration of the finer fraction” with no change in volume but a “relatively small and slow change in local hydraulic conductivity”.

4. Internal Stability Criteria

4.1. Shape Analysis Methods for Internal Stability Assessment

Kezdi [25] and Sherard [7] independently proposed theoretical methods to assess internal stability by splitting the gradation into a fine part and a coarse part (*i.e.*, $D_{15}/d_{85} = 4$) to evaluate the self-filtering ability of the soil. However, the split-gradation approaches were not substantiated by laboratory testing. From the outset of the USACE [26] filter experiments, Kenney and Lau [15] [16] studied the internal stability of sand and gravel

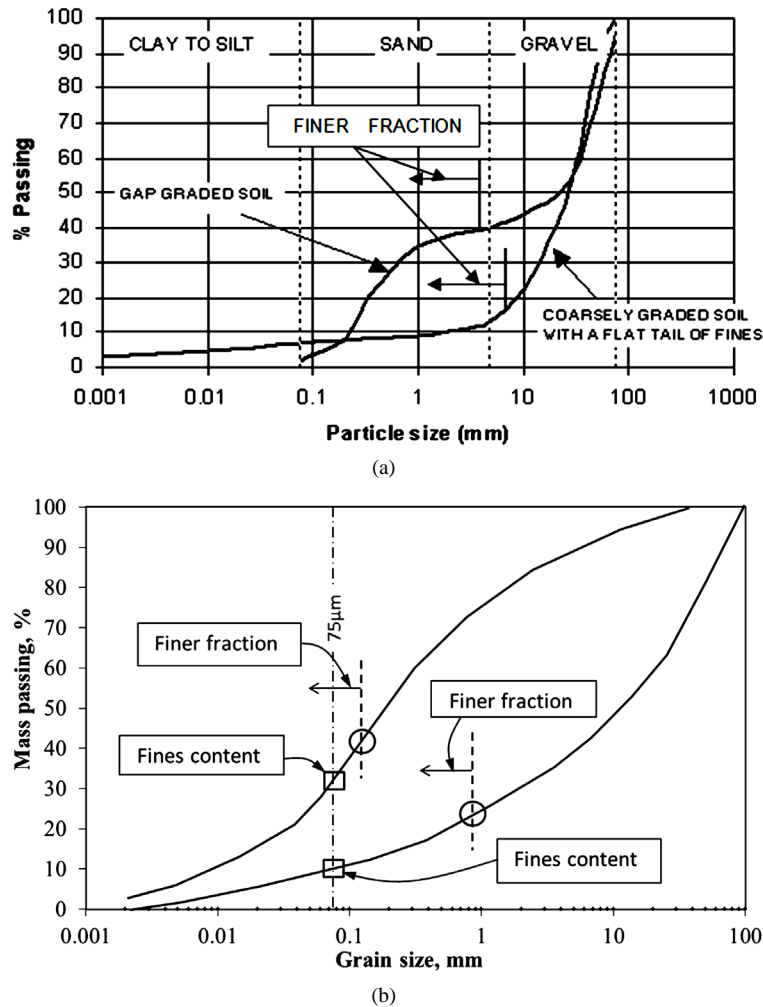


Figure 2. Determining the finer fraction: (a) Illustration reproduced from ICOLD [6] showing a gap-graded soil and coarsely graded soil; and (b) Schematic showing the application of the ICOLD finer-fraction procedure to fines-rich versus fines-poor glacial till gradations (after [13]).

specimens in a laboratory setting with permeameter experiments, and Li and Fannin [27] adapted it to include the Kezdi [25] split-gradation method. Burenkova [17] used a different approach to study suffusion susceptibility by dry mixing various fractions and identifying volume changes that occur when finer fractions are introduced. However, Wan and Fell [22] discovered that previous attempts to test the internal stability of soils did not include soils with silt or clay; most of the investigations were on cohesionless sand-gravel mixtures or coarse granular materials, so they conducted seepage tests on clay-silt-sand-gravel and silt-sand-gravel mixtures. Wan and Fell [22] subsequently found that the approach of Burenkova [17] provided satisfactory predictions when analyzing specimens that contain silt.

The approaches by Kenney and Lau [15] [16] and Burenkova [17], with the respective adaptations by Li and Fannin [27] and Wan and Fell [22] [28], are discussed further in the following sections.

4.2. The Kenney-Lau Method and Li-Fannin Adaptation

Based on tests of cohesionless sands and gravels that contain particles up to 100 mm without a silt fraction, Kenney and Lau [15] concluded that soils that experience a loss of fine-grained particles have unstable gradations and conversely that the gradation is stable where there is no loss of particles. Kenney and Lau [15] [16] then proposed a method for evaluating the potential for grading instability; they deduced stable versus unstable

gradations based on the shape of the particle size distribution with a limiting-shape curve of $H = 1.0F$. The method involves determining the mass fraction of particle sizes between D and $4D$ (denoted by H) and the passing weight at the particle size D (*i.e.*, F); a deficiency in the number of particles of a certain fraction (between D and $4D$) will potentially allow for the erosion of particles that are finer than D . For widely graded materials ($C_u > 3$), the evaluation range is passing weights of 0 to 20%, which is the maximum range for loose particles in such a soil according to Kenney and Lau [15]. Thus, a stability index H/F of less than one indicates that a soil is deficient in the finer fraction and is potentially internally unstable. The evolution of the Kenney and Lau approach is covered in Rönnqvist and Viklander [29].

Li and Fannin [27] proposed extending the approach of Kenney and Lau [15] [16] to include the criterion of Kezdi [25]. These methods are similar; both examine the slope of the grading curve over a certain length. As reported by Li and Fannin [27], the Kezdi criterion is incremental over the percentage that is finer by mass, whereas the Kenney-Lau criterion is incremental over the grain size. **Figure 3** shows the application of the Kenney-Lau method and Li-Fannin adaptation and how to generate the stability index $(H/F)_{\min}$ from the H:F-shape curve.

4.3. The Burenkova Method and Wan-Fell Adaptations

Burenkova [17], who tested cohesionless sand-gravel soils with $C_u = d_{60}/d_{10}$ values up to 200 and particle sizes up to 100 mm and some silt fractions (less than 10% fines), dry mixed a coarse fraction while gradually introducing a finer fraction. No net change to the volume of the sample indicated that the finer fraction was part of the loose particles and thus susceptible to suffusion. Conversely, an increase in volume would indicate that the finer fraction belongs to the soil skeleton and is therefore structural; thus, it is not susceptible to suffusion. Three soil grain sizes (*i.e.*, d_{90} , d_{60} and d_{15}) were identified, and a predictive method for assessing the suffusive or non-suffusive characteristics of soils were proposed by combining these sizes into factors of uniformity h' and h'' (*i.e.*, d_{90}/d_{15} and d_{90}/d_{60} , respectively), which define the boundaries for suffusive and non-suffusive soils (**Figure 4**) [17].

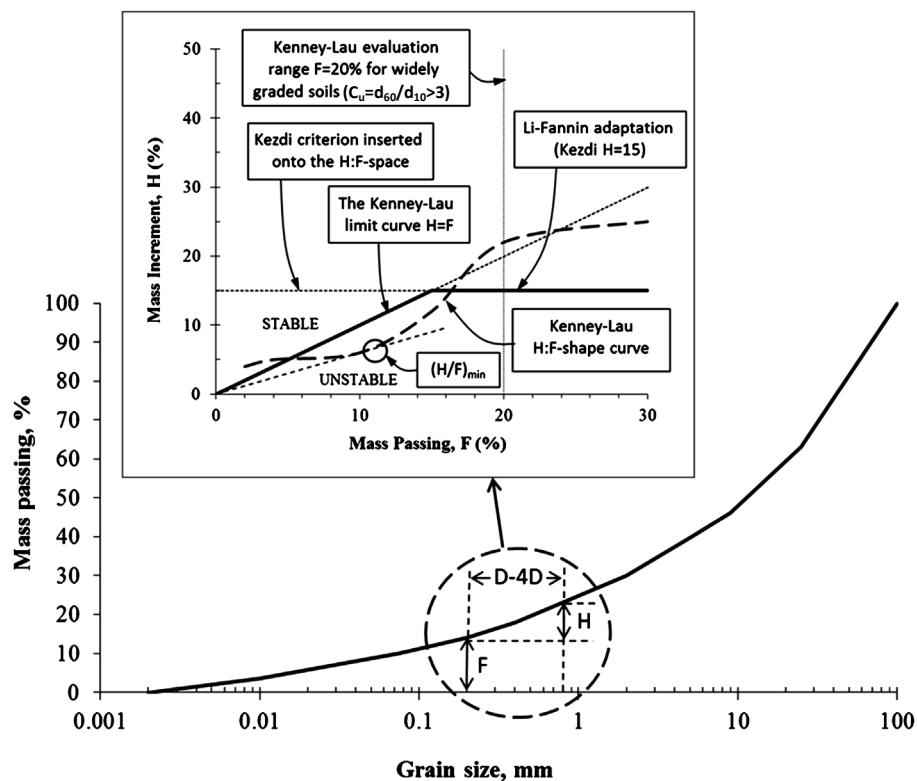


Figure 3. Illustration of the Kenney-Lau method. The inset shows the H:F-shape curve and stability index and the Li-Fannin adaptation (adapted after [15] [16] [27]).

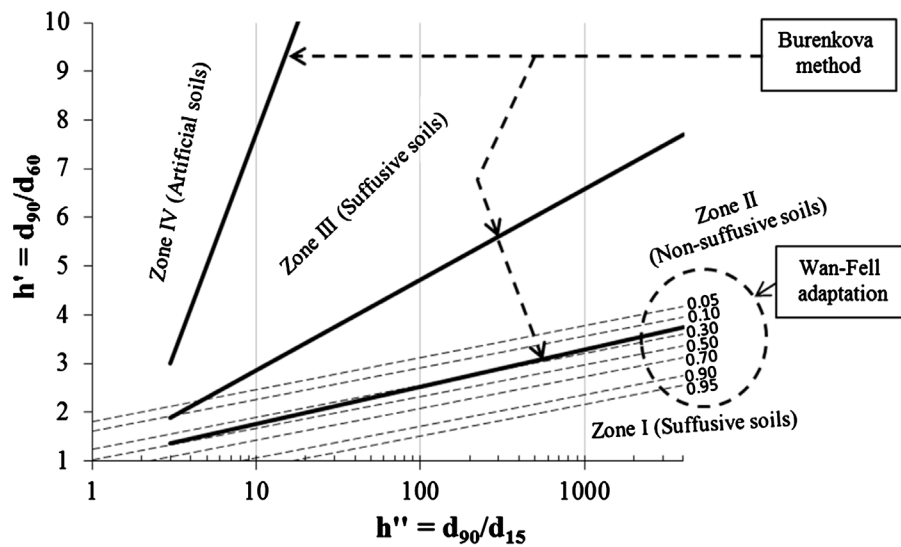


Figure 4. Illustration of the Burenkova method with the Wan-Fell adaptation with contours of the probability of internal instability superimposed (adapted after [17] [22]).

Based on downward and upward flow seepage tests on clay-silt-sand-gravel and silt-sand-gravel mixtures that are rich in fines, Wan and Fell [22] determined that the Burenkova method gave reasonable correlations to their seepage tests. They adapted the method to include a probabilistic approach that incorporated contours of the probability of internal instability (Figure 4). When the Wan-Fell [22] contours are superimposed over the Burenkova [17] boundaries and zones (Figure 4), the Wan-Fell adaptation is shown to partly cross over into the Burenkova non-suffusive zone.

Wan and Fell [28] subsequently proposed an alternative method for broadly graded soils. They found that gradations that are uniformly graded in the coarse fraction (*i.e.*, steep slope) and broadly graded in the finer fraction (*i.e.*, flat slope) were likely to be internally unstable but were not necessarily predicted to be by the Burenkova method. This alternative method uses the same characteristic D_{90}/D_{60} value for the coarser fraction but combines it with a value of D_{20}/D_5 for the finer fraction.

5. Database of Glacial Till Gradations

5.1. Experimental Database of Gradations

In a literature review of laboratory internal stability tests, five studies that involved glacial tills and laboratory suffusion tests were identified [13]. These were the investigations by Lafleur and Nguyen [8], Wan [9], Moffat *et al.* [10], Hunter *et al.* [11], and Lilja *et al.* [12], which all incorporated glacial till samples that were either related to, or directly sourced from, dam core zones or transitions.

Compiling these gradations results in an experimental database that includes 11 gradations (Figure 5), whose characteristics are summarized in Table 1; of these, seven gradations are internally unstable according to laboratory tests (*i.e.*, S7, S10, C-20, C-30, CG3, Mr3 and Mr19). Using seepage tests with a gradient of 10, Lafleur and Nguyen [8] found that cohesionless broadly graded glacial tills with fines content up to 12% (with D_{max} of 38 mm) were susceptible to suffusion, but tills with higher fines content were not susceptible (Table 1). Wan [9] found that when subjected to a constant gradient of 8, a glacial till with 20% fines (with D_{max} of 4.75 mm) is not susceptible to suffusion. Moffat and Fannin [10] [30] observed suffusive characteristics in a glacial soil with non-plastic fines up to 30% (with D_{max} of 20 mm). Furthermore, based on seepage tests, Lilja *et al.* [12] reported internal instability in glacial tills with fines between 25% to 35% (with D_{max} of 30 mm). While investigating global backward erosion, Hunter *et al.* [11] found that the coarse test grading CG3 experienced backward erosion but concluded that suffusion most likely indirectly influenced the process.

Characteristics of Gradations

The studied gradations comprise glacial till soils with the fines content (passing 0.075 mm when regraded on the

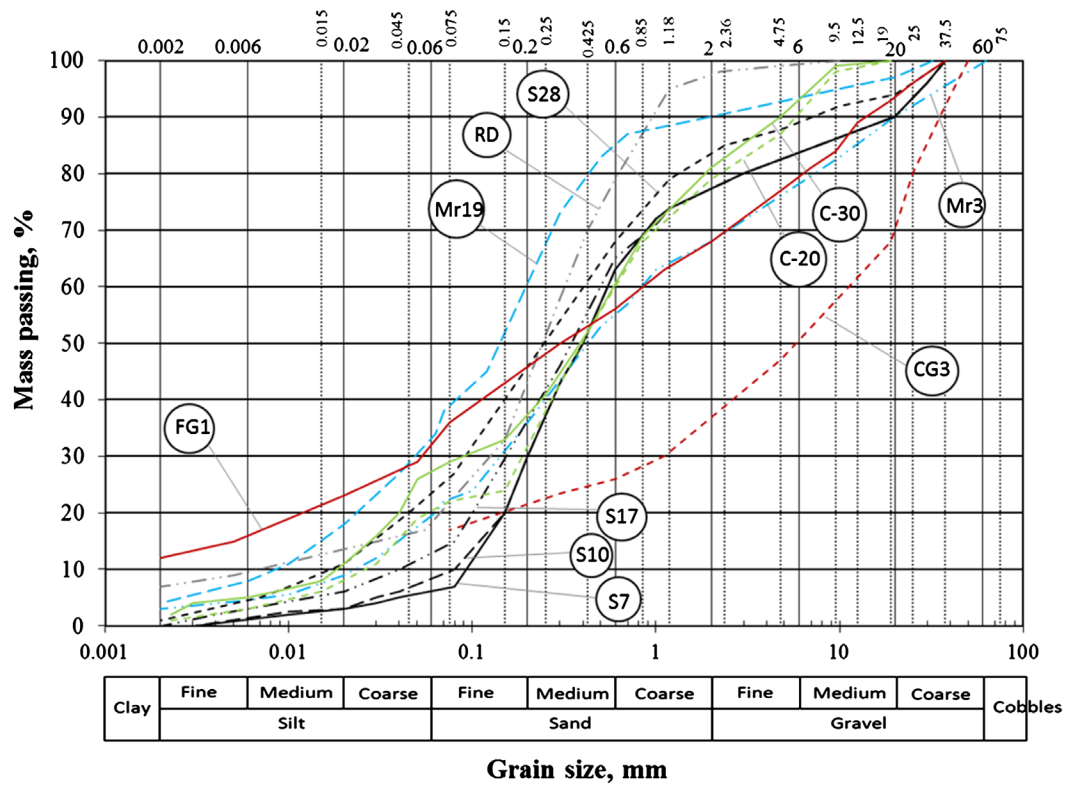


Figure 5. Compilation of glacial till gradations from laboratory internal stability tests (after [13]).

Table 1. Characteristics of gradations from the cores of existing dams.

Source	Gradation	D_{max} (mm)	Fines content (%) ^a	Finer fraction (%) ^b	$C_u = d_{60}/d_{10}$	Summary of test results
Lafleur and Nguyen [8]	S28	37.5	28 (36)	38	24	Stable
	S17	37.5	17 (20)	37	13	Stable
	S10	37.5	10 (12)	33	6	Unstable
	S7	37.5	7 (8)	25	6	Unstable
Wan [9]	RD	9.5	22 (23)	45	49	Stable
Moffat <i>et al.</i> [10]	C-20	19	20 (26)	20	20	Unstable
	C-30	19	30 (33)	35	30	Unstable
Hunter <i>et al.</i> [11]	FG1	37.5	33 (43)	40	425	Stable
	CG3	53	17 (36)	25	147	Unstable
Lilja <i>et al.</i> [12]	Mr3	63	22 (29)	32	40	Unstable
	Mr19	31.5	38 (41)	38	25	Unstable

^aMass passing 0.075 mm of the full sample; brackets indicate that it is regraded to #4 sieve (*i.e.*, 4.75 mm); ^bPoint of inflection on the gradation curve.

4.75 mm sieve) of 8% to 43% and coefficients of uniformity ($C_u = d_{60}/d_{10}$) of 6 to 425 (Table 1). Several of the gradations have finer fractions that exceed 35% (*i.e.*, gradations S28, S17, RD, FG1, and Mr19) and are thus potentially not susceptible to suffusion. This will be addressed in the analyses in the following sections.

5.2. Database of Existing Dams with Cores of Glacial Till

In a study of the possibility of extending the Kenney-Lau method [15] [16] to gradations that include a fraction

of non-cohesive silt, specifically glacial till, the gradations of the core soil of glacial till belonging to 74 existing dams were analyzed [14]. Performance monitoring data described in published and unpublished reports were used to identify 23 of the dams in which internal erosion has been documented; the other 51 dams have no records of deficiencies that can be reasonably attributed to internal erosion. Thus, the dams were sorted into 1) dams with the probable occurrence of internal erosion, and 2) dams with no observations that indicate internal erosion.

5.2.1. Reducing the Influence of the Filter

The comparative analysis was performed on dams within the same range of filter coarseness to minimize the influence of the filter (*i.e.*, filter D_{15}) on internal erosion and increase the influences of the core and a potential subordinate cause of internal erosion (e.g., core internal instability) [14].

Foster and Fell [31] advocate three empirical boundaries for soil retention: a No Erosion (NE) boundary, an Excessive Erosion (EE) boundary, and a Continuing Erosion (CE) boundary. A Some Erosion zone with base soil retention is located between the NE and EE boundaries. This zone, which varied between $D_{15} = 0.7$ mm and approximately 6 mm for the analyzed gradations in this study, was present in 44 of the 74 dams, thus distinguishing a group of dams within the same filter coarseness range [14].

5.2.2. Select Gradations for Analysis

Given that neither soils with excessive finer fraction nor glacial till with excessive fines content are susceptible to suffusion [6] [8], the population of dams was screened accordingly. Thirteen dams remained after screening out dams with finer content $> 35\%$ and fines content $> 30\%$ (based on the average values obtained from the soil's gradation envelope); these dams have thus gradations that are possibly susceptible to suffusion. Five are dams with performance history of internal erosion (*i.e.*, probable occurrence of internal erosion) (Table 2, Table 3). The gradation analyses established the most vulnerable gradation curve of the available grain size distributions for each dam (Figure 6, Table 2).

5.2.3. Characteristics of Gradations

The soils are cohesionless glacial tills with low to zero clay content and non-plastic or low-plasticity fines. Gradations denoted A, L, N, P and S represent dams considered to have a probable occurrence of internal erosion

Table 2. Characteristics of gradations from existing dam cores.

Source	Denotation	D_{\max} (mm)	Fines content (%) ^a	Finer fraction (%) ^b	$C_u = d_{60}/d_{10}$	Performance in terms of internal erosion
Rönnqvist and Viklander [14]	4	16	16 (21)	30	40	No observations ^c
	11	16	10 (11)	20	8	No observations ^c
	17	16	32 (35)	28	39	No observations ^c
	22	16	24 (28)	39	75	No observations ^c
	26	16	18 (21)	28	30	No observations ^c
	37	64	38 (54)	32	133	No observations ^c
	45	128	11 (15)	16	19	No observations ^c
	54	64	18 (35)	21	133	No observations ^c
	A	150	32 (53)	33	1357	Probable occurrence ^d
	L	20	19 (24)	35	60	Probable occurrence ^d
	N	150	20 (34)	28	200	Probable occurrence ^d
	P	16	12 (16)	35	32	Probable occurrence ^d
	S	180	11 (18)	35	53	Probable occurrence ^d

^aMass passing 0.075 mm of the full sample; brackets indicate that it is regraded to #4 sieve (*i.e.*, 4.75 mm); ^bPoint of inflection on the gradation curve; ^cNo observations to indicate internal erosion; ^dProbable occurrence of internal erosion.

Table 3. Summary of performance record in terms of internal erosion for dams with probable occurrence of internal erosion.

Source	Denotation	Dam and year of completion	Country	Performance record
Rönnqvist and Viklander [14]	A	Hytteljuvet (1965)	Norway	Muddy discharge upon first filling and subsequently over time, and a sinkhole incident in 1972. Exploratory borings showed locally large flows [32] [33].
	L	Lövön (1973)	Sweden	Sinkhole incidents in 1983 and 1986. Investigations showed a loss of fines in the core, loose zones, cavities and elevated pore pressures, as well as signs of suffused and piped core materials and clogging of fines against the filter face [4] [34].
	N	Viddalsvattn (1971)	Norway	Increased seepage flow with muddy discharge upon first filling and subsequently over time and a sinkhole incident in 1973 [35].
	P	Porjus (1975)	Sweden	Sinkhole incident upon first filling and sinkhole incidents in 1979, 1985 and 1993 with increased seepage flow. Investigations showed erosion of the core and high pore pressures in the filter [4] [36].
	S	Songa (1962)	Norway	Muddy discharge in 1991 and settlement on the crest. Investigations showed loose zones in the core and zones of water loss [37].

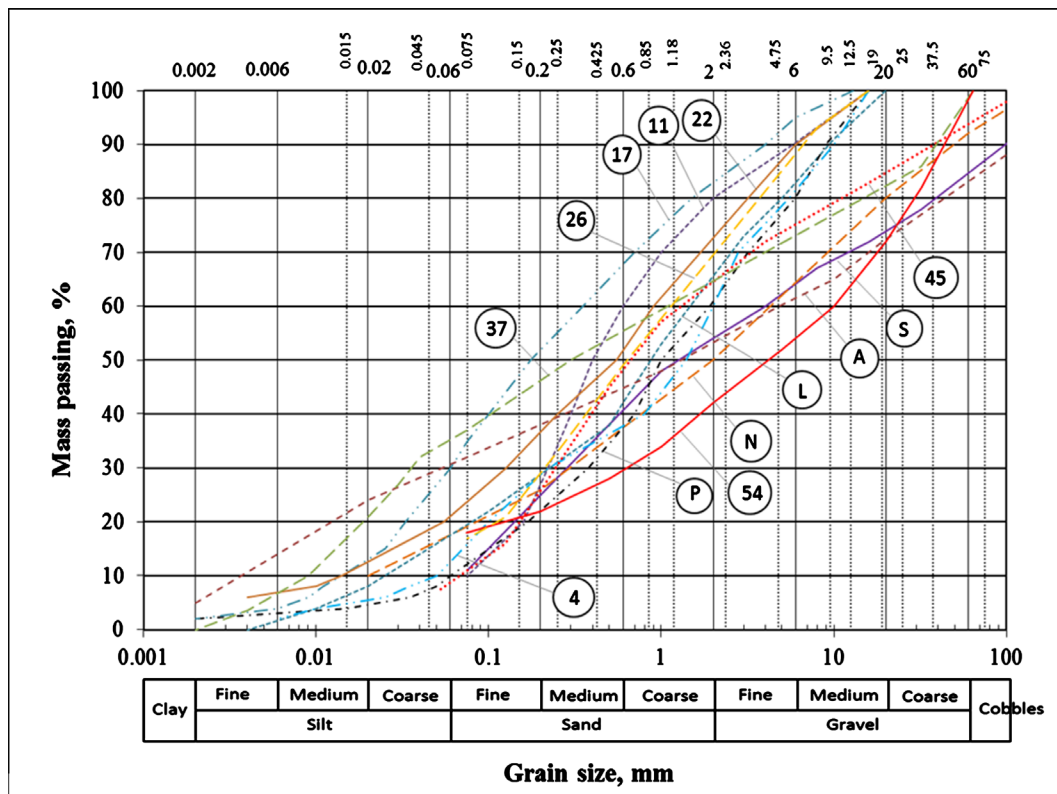


Figure 6. Compilation of glacial till gradations from cores of existing dams, some of which have experienced internal erosion (after [14]).

(Table 2). Details of the performance record for these dams reveals incidents of high piezometric water levels, increased seepage flow, and muddy discharge, in many cases accompanied by sinkhole activity; all of these are indications of probable occurrence of internal erosion (Table 3).

The fines content (passing 0.075 mm when regraded on the 4.75 mm sieve) of the glacial tills varies from 11% to 54% with coefficients of uniformity ranging from 8 to 1357 (Table 2). One of the gradations has a finer fraction greater than 35% (39%; gradation 22) and is thus potentially not susceptible to suffusion. This will be addressed in the analyses in the following sections.

6. Empirical Analysis of Internal Instability Using Existing Methods

6.1. The Kenney-Lau Approach

The Kenney-Lau method [15] [16] evaluates the potential for internal stability by analyzing the shape of the finer end of the gradation curve. The Li-Fannin adaptation [27] incorporates the Kezdi [25] split-gradation method. The H:F-shape curves of the most vulnerable core gradations are shown in Figure 7, and the corresponding stability indexes (*i.e.*, H/F_{min}) are shown in Figure 8(a). The stability index is the smallest value along the H:F curve within the evaluation range is mass passing 0 to 20% (for widely graded materials, $C_u = d_{60}/d_{10} > 3$), as indicated in Figure 7 and Figure 8).

A summary of the analyses (Table 4) shows that the Kenney-Lau method identifies 75% of the unstable gradations and that 56% of the potentially unstable gradations are gradations that tested or performed as unstable (Figure 8(a)). Disregarding the gradations with finer fraction > 35% (not susceptible to suffusion), 82% of the unstable gradations were identified. The equivalent values for the Li-Fannin adaptation are 67% and 67%, respectively (Figure 8(b), Table 4).

6.2. The Burenkova Approach

The Burenkova method [17] evaluates the potential for internal instability using a characteristic value for the slope of the coarser fraction (D_{90}/D_{60}) and the overall slope of the gradation curve (D_{90}/D_{15}). The Wan-Fell adaptation [22] incorporates a probabilistic approach within the same framework of the grain size ratio. The distribution of gradations from the Burenkova method is given in Figure 9, and the distribution from the Wan-Fell adaptation is shown in Figure 10.

A summary of the analyses (Table 4) of the most vulnerable core gradations shows that the Burenkova method identifies 58% of the unstable gradations and that 47% of the potentially unstable gradations are gradations which have tested or performed as unstable (Figure 9). The equivalent values for the Wan-Fell adaptation are 8% and 50%, respectively (Figure 10, Table 4) for a greater than 5% probability of internal instability (for silt-sand-gravel soils and clay-silt-sand-gravel soils with limited clay contents and plasticity).

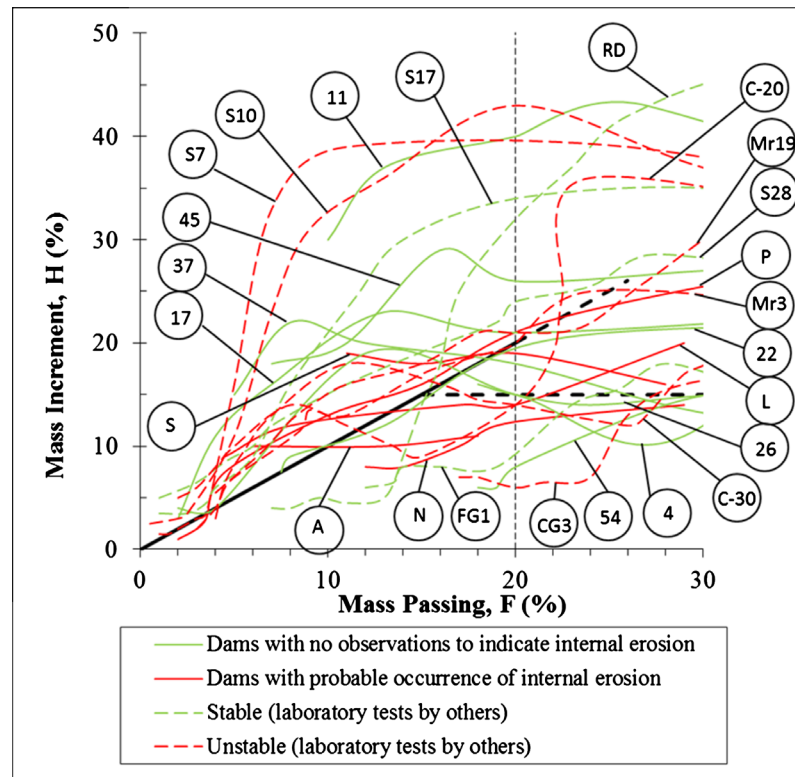


Figure 7. H:F-shape curves obtained by applying the Kenney-Lau method.

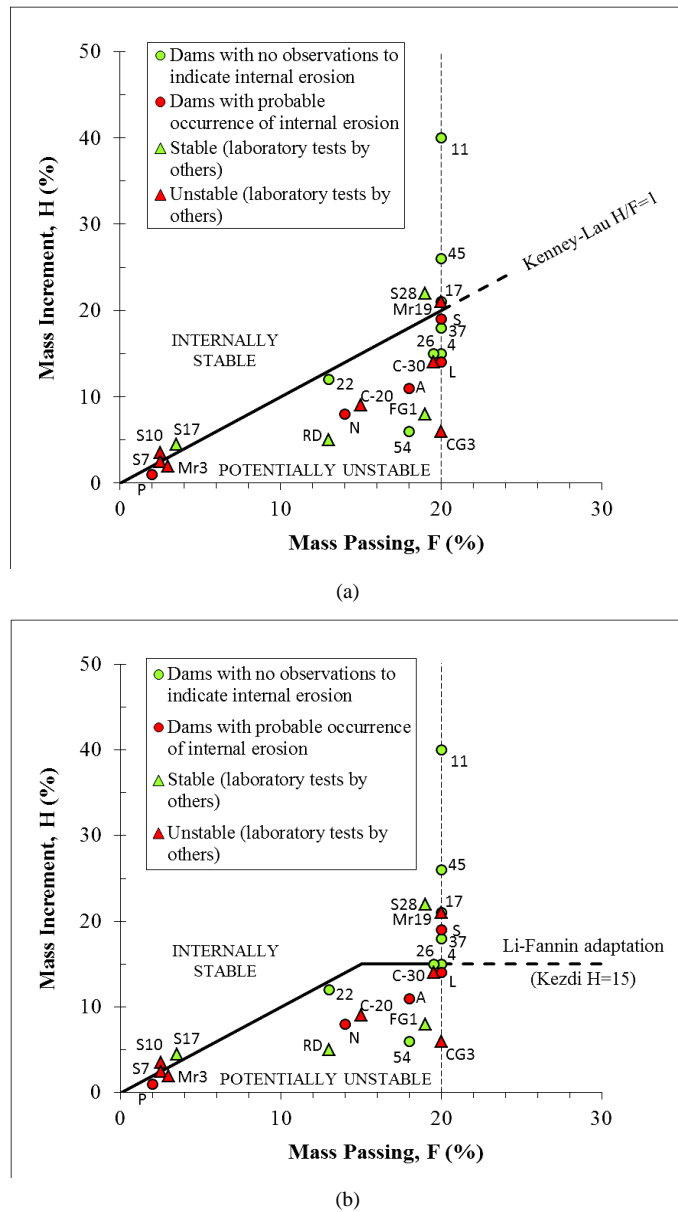


Figure 8. Stability indexes $(H/F)_{min}$ compared to the boundary of (a) the Kenney-Lau method and (b) the Li-Fannin adaptation.

Table 4. Summary of test results from gradation analyses of glacial till core specimens.

Empirical Criteria	Identified unstable gradations (%)	Unstable gradations not identified	Potentially unstable with unstable performance (either in laboratory tests or <i>in-situ</i> at dams)
Kenney-Lau method [15] [16]	75 (82 ^a)	S7, S10, Mr19	56 (69 ^a)
Li-Fannin adaptation [27]	67 (73 ^a)	S7, S10, Mr19, S	67 (89 ^a)
Burenkova method (zone I or III) [17]	58 (55 ^a)	S7, S10, Mr3, CG3, A	47 (55 ^a)
Wan-Fell adaptation (>5% probability) [22]	8 (9 ^a)	S7, S10, Mr3, Mr19, C-20, C-30, A, L, N, P, S	50 (50 ^a)
Wan-Fell alternative method [28]	0	S7, S10, Mr3, Mr19, C-20, C-30, A, L, P ^b	0

^aResults when gradations with finer fraction > 35% are excluded (i.e., S17, S28, RD, FG1, Mr19 and 22); ^bGradations RD, FG1, CG3, S, N, 11, 26 and 54 are not included because gradation data on minus #200 sieve are not available.

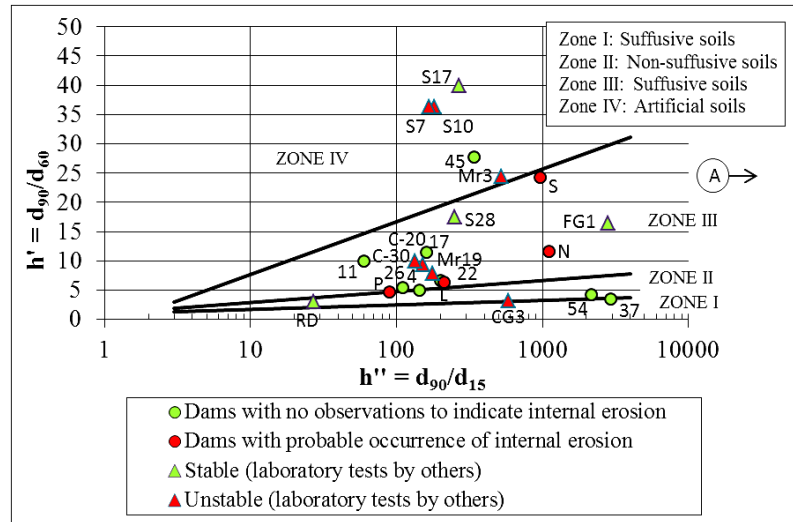


Figure 9. Distribution of gradations obtained by applying the Burenkova method.

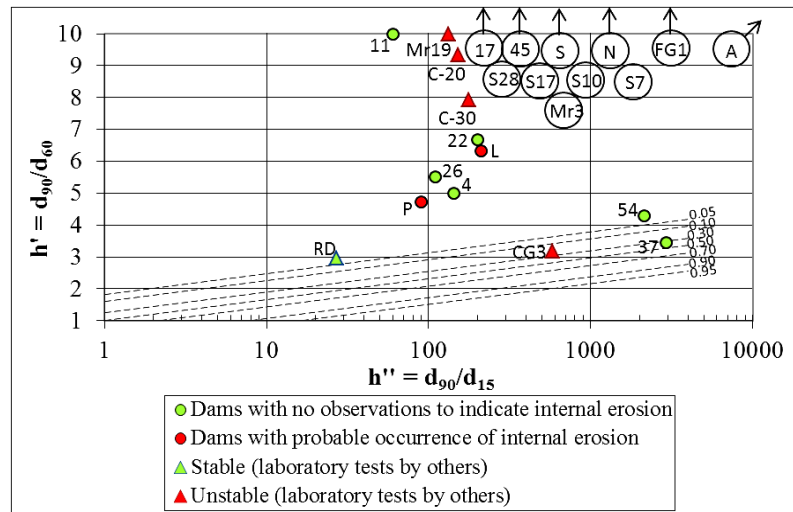


Figure 10. Distribution of gradations obtained by applying the Wan-Fell adaptation with contours of the probability of internal instability.

6.3. The Wan-Fell Alternative Method

Recognizing that the Burenkova approach may not provide accurate predictions for gradations that are uniform in the coarse fraction and broad in the finer fraction, Wan and Fell [28] proposed that the potential for internal instability in these broadly graded soils be evaluated using the same characteristic D_{90}/D_{60} value for the coarser fraction but with a value of D_{20}/D_5 for the finer fraction. The distribution of gradations is shown in Figure 11.

A summary of the analyses (Table 4) for the most vulnerable core gradation shows that the Wan-Fell alternative method predicts that none of the gradations are potentially unstable (located in the unstable or transition region).

7. Discussion

Although the soils investigated by Kenney and Lau [15] are cohesionless sand and gravels without fines, experimental observations indicate that the Kenney-Lau method may also apply to soils that have a fraction of non-plastic silt [10] [30] [38]. In addition, the Li and Fannin [27] adaptation of the Kenney-Lau approach to broadly graded soils with some fines appears to be more reliable [38] [39] and provide a less conservative analysis

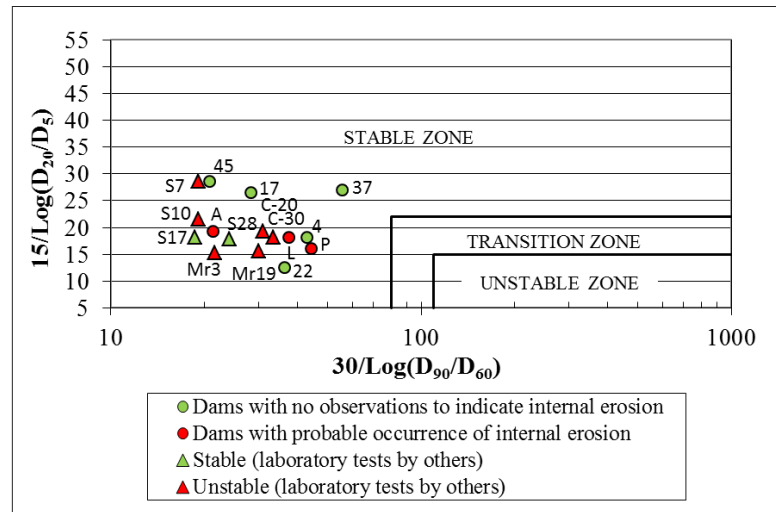


Figure 11. Distribution of gradations obtained by applying the Wan-Fell alternative method for broadly graded soils (gradations RD, FG1, CG3, S, N, 11, 26 and 54 are not included due to data on minus #200 sieve are not available).

[14]. However, Burenkova [17] tested some silt-sand-gravel soils, and Wan and Fell [22], who adapted the Burenkova method, focused on broadly graded soils that contain silt and clay.

The comparative analysis indicates that both the Kenney-Lau approach and the Burenkova method have merit in terms evaluating the internal stability of glacial till gradations, and a closer analysis indicates that the Kenney-Lau method has better predictive ability, particularly with its Li-Fannin adaptation (Table 4). However, the Wan-Fell adaptation [22] (Figure 10) and the Wan-Fell alternative method [28] (Figure 11) appear to be less successful for glacial till gradations. Figure 12 compiles the 20 gradations that Wan-Fell tested and based their methods on; unstable results in the UNSW tests are shown as red lines in the particle size distributions, while stable are shown as green lines. Although the tested soils include a wide range of gradations, they are mostly gap-graded or steep-sloped in the coarser fraction and flat in the finer, which is relatively uncharacteristic of the typically smooth gradations of the well-graded glacial tills investigated in this paper (compare with Figure 5 and Figure 6). This may indicate the potentially limited predictive ability of these methods for glacial till gradations.

Interestingly, neither the Kenney-Lau approach nor the Burenkova successfully identifies the unstable gradations S7 and S10 that were tested by Lafleur and Nguyen [8] (Figure 5, Table 4). Lafleur and Nguyen [8] argued that a glacial till sample would gradually become more susceptible to suffusion with decreasing fines content (which increases the upward concavity of the grading, thus potentially making it unstable). They found that over time, the fines-poor samples ultimately showed a loss of head near the filter interface (Figure 13(a)), whereas the fines-rich samples exhibited a uniform head loss through the sample (Figure 13(b)). The head loss in the fines-poor gradations was caused by the accumulation of migrating particles from clogging, and the migration of particles was possible due to internal instability. In contrast, the fines-rich samples behaved the same over time and showed no changes in gradation; thus, they were internally stable. Lafleur and Nguyen [8] used a relatively fine-grained filter (*i.e.*, filter paper with an opening size of 0.011 mm, which corresponds approximately to $D_{15} = 0.1$ mm) as the interface with the glacial till. This would result in a “closed system that prevents loss of particles” [15]. In their internal stability tests, Kenney and Lau [15] [16] abandoned the closed system for an open system to allow unrestricted seepage from the base through the filter. They found that the open system facilitated the monitoring and the subsequent interpretation of the tests. Furthermore, Kenney and Lau [15] usually found that unstable soil exhibited a top transition zone, a central homogenous zone, and a bottom transition zone [15]. Thus, Kenney and Lau [15] concluded that any coarsening of the top transition zone proved the existence of loose movable particles, whereas Lafleur and Nguyen [8] interpreted head loss against the filter (due to accumulation of migrating fines) and increase in fines content as indications of internal instability. In the specimens determined as unstable by Lafleur and Nguyen [8], namely the glacial tills with fines less than 12% (at a D_{max} of 38 mm), the fines content increased at the most from an initial 4% to 8% and for the specimen S10 analyzed herein from 10% to 13% (Figure 13(c)), thus a relatively small change. It is possible that the methods

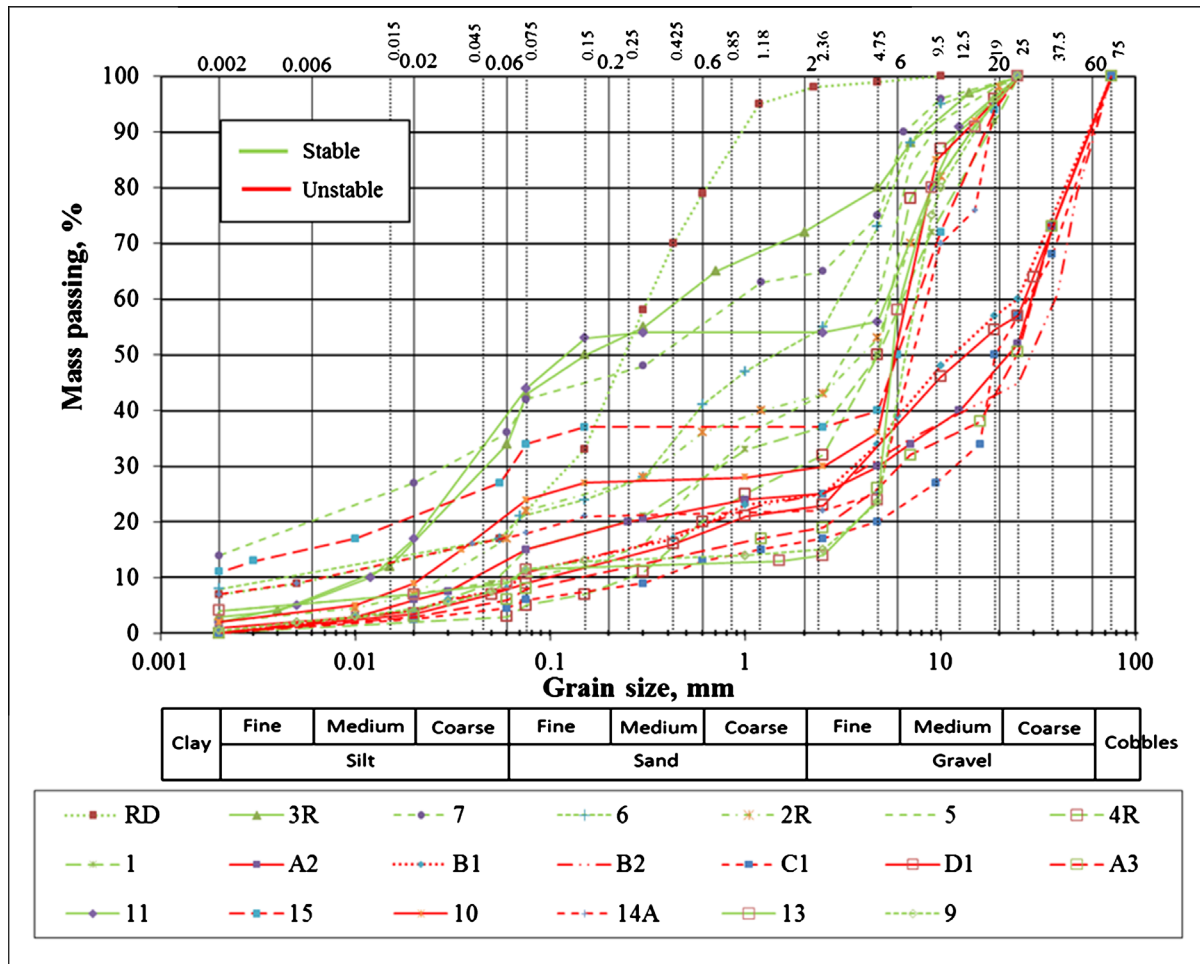


Figure 12. Compilation of gradations tested by Wan-Fell and UNSW (adapted after [9]).

investigated in this study are too crude to identify instability from such a minute change in gradation.

An inspection of the shapes of the gradations investigated in this study reveals that S17, S28, RD, FG1, Mr19 and 22 (Figure 5, Figure 6) have finer fraction in excess of 35% and thus are potentially not susceptible to suffusion (Table 1 and Table 2). When these samples are excluded, the predictive ability of the methods generally increases, most notably for the Li-Fannin adaptation because it identifies 73% of the unstable gradations and determines that 89% of the potentially unstable gradations are gradations that have tested or performed as unstable (Table 4). Figure 14 shows a plot of the stability indexes $(H/F)_{\min}$ when gradations with finer fractions $> 35\%$ are excluded.

8. Conclusion

This paper investigates the applicability of available empirical methods for assessing the internal stability of glacial tills. A database of 24 gradations was compiled. The database incorporates experimental gradations from laboratory studies in the literature and selected gradations from existing dams, some of which have experienced internal erosion. Internal instability may cause suffusion, which is an initiation mechanism of internal erosion. Two approaches are used to evaluate the internal stability: the Kenney-Lau method [15] [16], which analyses the shape of the gradation curve; and the Burenkova method [17], which uses characteristic values of the slope of the gradation (factors of uniformity). The shape analysis of the gradations and the comparative analysis of the methods presented in this study indicate that both the Kenney-Lau method and the Burenkova method have merit, but a closer analysis indicates that the Kenney-Lau method has relatively better predictive ability based on the glacial till gradations analyzed in this study; when the Li-Fannin [27] adaptation is used, 73% of the unstable

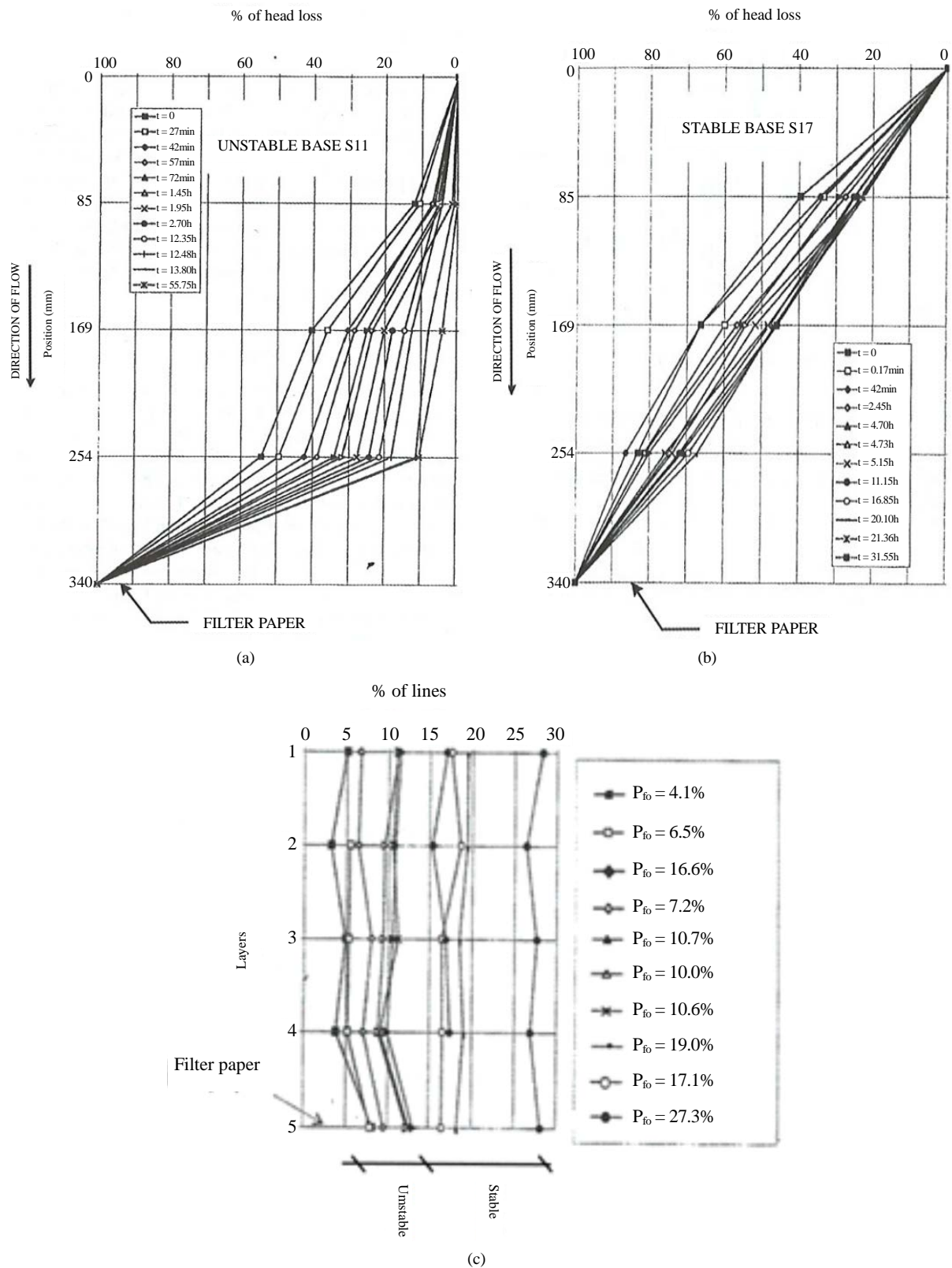


Figure 13. Suffusion tests by Lafleur-Nguyen showing head losses over time for (a) internally unstable base S11, (b) internally stable base S17, and (c) change in fines content for stable and unstable till specimens (adapted after [8]).

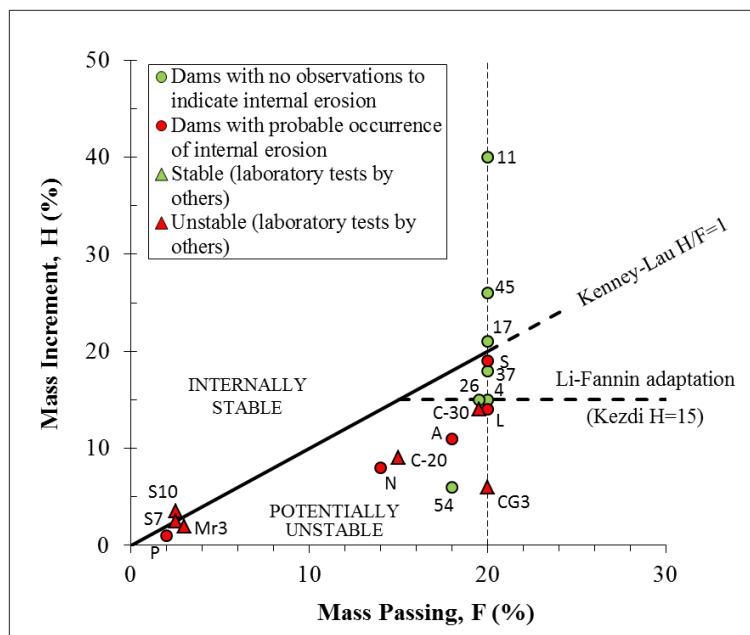


Figure 14. Plot of stability indexes $(H/F)_{\min}$ when excluding gradations with finer fraction > 35%.

gradations are identified and it determines that 89% of the potentially unstable gradations are gradations that tested or performed unstable (Figure 14).

Acknowledgements

The research presented was carried out as part of the “Swedish Hydropower Centre-SVC”. SVC has been established by the Swedish Energy Agency, Elforsk and Svenska Kraftnät together with Luleå University of Technology, the Royal Institute of Technology, Chalmers University of Technology and Uppsala University.

The authors acknowledge with gratitude the financial support received from WSP Sweden.

References

- [1] Bernell, L. (1976) Control of Leakage through Dams Founded on Glacial Till Deposits. *Proceedings of 12th ICOLD Congress*, International Commission on Large Dams, Mexico, 937-950.
- [2] Bernell, L. (1982) Experiences of Wet Compacted Dams in Sweden. *Proceedings of 14th ICOLD Congress*, International Commission on Large Dams, Rio de Janeiro, 421-431.
- [3] Foster, M., Fell, R. and Spannagle, M. (2000) The Statistics of Embankment Dam Failures and Accidents. *Canadian Geotechnical Journal*, **37**, 1000-1024. <http://dx.doi.org/10.1139/t00-030>
- [4] Nilsson, Å., Ekström, I. and Söder, C. (1999) Sinkholes in Swedish Embankment Dams. *Elforsk Report*, **99**, 34.
- [5] Rönnqvist, H. (2009) Long-Term Behaviour of Internal Erosion Afflicted Dams Comprising Broadly Graded Soils. *Dam Engineering*, **20**, 149-197.
- [6] ICOLD (2013) Internal Erosion of Existing Dams, Levees and Dykes, and Their Foundations. In: Bridle, R. and Fell, R., Eds., *Bulletin 164, Volume 1: Internal Erosion Processes and Engineering Assessment*, International Commission on Large Dams, Paris.
- [7] Sherard, J.L. (1979) Sinkholes in Dams of Coarse, Broadly Graded Soils. *Proceedings of 13th ICOLD Congress*, Vol. II, International Commission on Large Dams, India, 25-35.
- [8] Lafleur, J. and Nguyen, P.H. (2007) Internal Stability of Particles in Dam Cores Made of Cohesionless Broadly Graded Moraines. *Internal Erosion of Dams and Their Foundations*, Taylor & Francis, UK, 151-158.
- [9] Wan, C.F. (2006) Experimental Investigations of Piping Erosion and Suffusion of Soils in Embankment Dams and Their Foundations. Ph.D. Thesis, University of New South Wales, Sydney.
- [10] Moffat, R., Fannin, R.J. and Garner, S. (2011) Spatial and Temporal Progression of Internal Erosion in Cohesionless

- Soil. *Canadian Geotechnical Journal*, **48**, 399-412. <http://dx.doi.org/10.1139/T10-071>
- [11] Hunter, G., Fell, R. and Topham, C. (2012) Backward Erosion Piping: What Are the Chances of That? *Proceedings of ANCOLD 2012*, Perth, 24-28 October 2012.
- [12] Lilja, H.M., Rother, M. and Ravaska, O.T. (1998) Filter Material Study for an Earth Dam Project. In: Berga, L., Ed., *Dam Safety*, Balkema, 825-832.
- [13] Rönnqvist, H. and Viklander, P. (2014) Laboratory Testing of Internal Stability of Glacial Till, a Review. *Electronic Journal of Geotechnical Engineering*, **19**, 6315-6336.
- [14] Rönnqvist, H. and Viklander, P. (2014) Extending the Kenney-Lau Method to Dam Core Soils of Glacial Till. *Geotechnical Research*, **1**, 73-87.
- [15] Kenney, T.C. and Lau, D. (1985) Internal Stability of Granular Filters. *Canadian Geotechnical Journal*, **22**, 215-225. <http://dx.doi.org/10.1139/t85-029>
- [16] Kenney, T.C. and Lau, D. (1986) Internal Stability of Granular Filters: Reply. *Canadian Geotechnical Journal*, **23**, 420-423. <http://dx.doi.org/10.1139/t86-068>
- [17] Burenkova, V.V. (1993) Assessment of Suffusion in Non-Cohesive and Graded Soils. In: Brauns, J., Schuler, U. and Heibum, M., Eds., *Proceedings of the 1st International Conference "Geo-Filters", Filters in Geotechnical Engineering*, Balkema, 357-360.
- [18] ICOLD (1989) Moraine as Embankment and Foundation Material—State of the Art. Bulletin 69, International Commission on Large Dams, Paris.
- [19] Milligan, V. (2003) Some Uncertainties in Embankment Dam Engineering. *Journal of Geotechnical and Geoenvironmental Engineering, ASCE*, **129**, 785-797. [http://dx.doi.org/10.1061/\(ASCE\)1090-0241\(2003\)129:9\(785\)](http://dx.doi.org/10.1061/(ASCE)1090-0241(2003)129:9(785))
- [20] Vaughan, P.H. and Soares, H.F. (1982) Design of Filters for Clay Cores of Dams. *Journal of the Geotechnical Engineering, ASCE*, **108**, 17-31.
- [21] Sherard, J.L. and Dunnigan, L.P. (1989) Critical Filters for Impervious Soils. *Journal of Geotechnical Engineering, ASCE*, **115**, 927-947. [http://dx.doi.org/10.1061/\(ASCE\)0733-9410\(1989\)115:7\(927\)](http://dx.doi.org/10.1061/(ASCE)0733-9410(1989)115:7(927))
- [22] Wan, C.F. and Fell, R. (2004) Experimental Investigation of Internal Instability of Soils in Embankment Dams and Their Foundation. UNICIV Report No. 429, The University of New South Wales, Kensington.
- [23] Skempton, A.W. and Brogan, J.M. (1994) Experiments on Piping in Sandy Gravels. *Géotechnique*, **44**, 449-460. <http://dx.doi.org/10.1680/geot.1994.44.3.449>
- [24] Garner, S.J. and Sobkowicz, J.C. (2002) Internal Instability in Gap-Graded Cores and Filters. *Proceedings of 2002 Annual CDA Conference*, Canadian Dam Association, Victoria.
- [25] Kezdi, A. (1979) Soil Physics—Selected Topics. Elsevier Scientific Publishing Co., Amsterdam, 160 p.
- [26] USACE (1953) Filter Experiments and Design Criteria. Technical Memorandum No. 3-360, Waterways Experiment Station, Vicksburg.
- [27] Li, M. and Fannin, R.J. (2008) Comparison of Two Criteria for Internal Stability of Granular Soil. *Canadian Geotechnical Journal*, **45**, 1303-1309. <http://dx.doi.org/10.1139/T08-046>
- [28] Wan, C.F. and Fell, R. (2008) Assessing the Potential of Internal Instability and Suffusion in Embankment Dams and Their Foundations. *Journal of Geotechnical and Geoenvironmental Engineering*, **134**, 401-407. [http://dx.doi.org/10.1061/\(ASCE\)1090-0241\(2008\)134:3\(401\)](http://dx.doi.org/10.1061/(ASCE)1090-0241(2008)134:3(401))
- [29] Rönnqvist, H. and Viklander, P. (2014) On the Kenney-Lau Approach to Internal Stability Evaluation of Soils. *Geomaterials*, **4**, 129-140.
- [30] Moffat, R. and Fannin, R.J. (2011) A Hydromechanical Relation Governing Internal Stability of Cohesionless Soil. *Canadian Geotechnical Journal*, **48**, 413-424. <http://dx.doi.org/10.1139/T10-070>
- [31] Foster, M.A. and Fell, R. (2001) Assessing Embankment Dam Filters That Do Not Satisfy Design Criteria. *Journal of Geotechnical and Geoenvironmental Engineering*, **127**, 398-407. [http://dx.doi.org/10.1061/\(ASCE\)1090-0241\(2001\)127:5\(398\)](http://dx.doi.org/10.1061/(ASCE)1090-0241(2001)127:5(398))
- [32] Wood, D., Kjaernsli, B. and Höeg, K. (1976) Thoughts Concerning the Unusual Behavior of Hyttejuvet Dam. *Proceedings of ICOLD 12th Congress*, International Commission on Large Dams, Mexico, 391-414.
- [33] Sherard, J.L. (1973) Embankment Dam Cracking. In: Hirschfeld, R.C. and Poulos, S.J., Eds., *Embankment-Dam Engineering (Casagrande Volume)*, John Wiley, New York, 324-328.
- [34] Ericsson, J. and Jender, M. (1998) Documentation and Investigation of Damages in Lövön Dam. Master's Thesis, Luleå University of Technology, Luleå.
- [35] Vestad, H. (1976) Viddalsvatn Dam a History of Leakages and Investigations. *Proceedings of 12th ICOLD Congress*, International Commission on Large Dams, Mexico, 369-390.

- [36] Bartsch, M., Bono, N., Nilsson, Å. and Norstedt, U. (2006) Alternative Measures to Improve the Resistance Against Internal Erosion—Upgrading of the Suorva and the Porjus Rockfill Dams. *Proceedings of ICOLD 22nd Congress*, International Commission on Large Dams, Barcelona, 207-228.
- [37] Torblaa, I. and Rikartsen, C. (1997) Songa, Sudden Variations of the Leakage in a 35 Years Old Rockfill Dam. *Proceedings of 19th ICOLD Congress*, International Commission on Large Dams, Florence, 255-267.
- [38] Li, M., Fannin, R.J. and Garner, S.J. (2009) Application of a New Criterion for Assessing the Susceptibility to Internal Erosion. *Proceedings of CDA 2009*, Canadian Dam Association, Whistler, 3-8 October 2009.
- [39] Li, M., Fannin, R.J. and Anderlini, C. (2014) Assessing Performance of a Potentially Internally Unstable Filter. *Proceedings of CDA 2014*, Canadian Dam Association, Banff, 4-9 October 2014.

Notations

D: grain size (mm);

F: amount of mass passing at grain size D (%);

H: mass increment between D and 4D (%);

D_{\max} : maximum particle size of gradation (mm);

C_u : coefficient of uniformity, d_{60}/d_{10} ;

$(H/F)_{\min}$: stability index, defined by the smallest value of H/F, for $0 < F \leq 20\%$ in soil with a widely graded coarse fraction and $0 < F \leq 30\%$ in soils that are narrowly graded.

Evaluation of the Impact of Truck Overloading on Flexible Compacted Gravel Lateritic Soil's Pavements by FEM with Cast3M[®]

Fatou Samb¹, Meissa Fall¹, Yves Berthaud², Farid Bendboudjema³

¹Laboratoire de Mécanique et Modélisation, UFR Sciences de l'Ingénieur, Université de Thiès, Thiès, Sénégal

²Sorbonne Universités, UPMC Univ Paris 06, UMR 7190, d'Alembert, F-75005, Paris, France

³Laboratoire de Mécanique et de Technologie, Ecole Normale Supérieure de Cachan, Cachan, France

Email: fatou.samb@univ-thies.sn

Received 25 September 2014; revised 25 October 2014; accepted 18 November 2014

Copyright © 2015 by authors and Scientific Research Publishing Inc.

This work is licensed under the Creative Commons Attribution International License (CC BY).

<http://creativecommons.org/licenses/by/4.0/>



Open Access

Abstract

Within the framework of a FEM of the nonlinear behavior of lateritic pavement of Senegal, the effect of truck overloading is studied to estimate its impact on the deformability of road pavement on compacted gravel lateritic soils. For that purpose, various loading conditions were tested to measure the impact on the critical response parameters of road pavement design. The implementation of the models was realized with Cast3M[®]. This study allowed us to point out that the observed variations are linear and would help to plan in advance the impact of axle overloads for a better evaluation within the framework of the mechanistic (M. E.) design of pavements.

Keywords

FEM, Axle Overload, Nonlinear Behavior, Gravel Lateritic Soil

1. Introduction

The regulation number 14/2005/CM/UEMOA of WAEMU (*West African Economic and Monetary Union*) of December 16th, 2005 concerning the harmonization of standards and control procedures of truck volumes, weights and axle loads of heavy goods vehicles in the member states of the Union, set the axle load to 12 tons for a single axle with dual-wheels (Uemoa, 2005 [1]). However, recent studies showed that this recommended official load is far from being respected. Indeed, 60% - 70% of heavy trucks are overloaded and have significant

How to cite this paper: Samb, F., Fall, M., Berthaud, Y. and Bendboudjema, F. (2015) Evaluation of the Impact of Truck Overloading on Flexible Compacted Gravel Lateritic Soil's Pavements by FEM with Cast3M[®]. *Geomaterials*, 5, 19-24.
<http://dx.doi.org/10.4236/gm.2015.51002>

contribution in the degradation of roads. The objective of this study is to determine the critical response parameters of lateritic roads materials submitted to various conditions of axle overload. The standard axle load is 130 kN (13 tons) for a single axle with dual-wheels (Bceom-Cebtp, 1984 [2]). The reference load is uniformly distributed on two circles whose centers are from 37.5 cm away from each other. The calculation of the stresses and the strains is done for a typical load of 6.5 tons exercising a vertical pressure q uniformly distributed on two circles with: $a = 12.5$ cm; $l = 3 \times a = 37.5$ cm and $q = 6.62$ bars. The reference load for the calculations is represented by the **Figure 1**.

The reference axle is varied from 13 to 20 tons to take into account the overloading. The effect of a single wheel is tested with a tire pressure of 0.662 MPa for the load of 13 tons and respectively 0.764 MPa, 0.917 MPa and 1.019 MPa respectively for axle loads of the 15, 18 and 20 tons (Samb, 2014 [3]).

2. Geometry, Materials and Algorithm of Calculations

The structure consists of a 80 mm thick bituminous concrete, a 200 mm thick base layer of lateritic gravels treated or not, a 250 mm thick subbase of untreated lateritic gravels and of a sandy subgrade of infinite thickness. The materials of the asphalt and subgrade layer are considered linear elastic. The base and the subbase has a nonlinear elastic behavior. To take into account this non-linearity, the elastic modulus is replaced by a resilient modulus which depends on the stress level. Several formulations were suggested by using various terms of stresses (Lekarp, Isacsson, and Dawson, 2000 [4]; Kim, 2007 [5]) and showed that the models proposed by Uzan (1985) [6] and the NCHRP (2004) [7] allow to take into account the behavior of granular soils as well as fine soils. Triaxial test results on the gravel lateritic soils of Ngoundiane showed that Uzan model give the best correlations and so, the model parameters was determined for these soils.

The Uzan model expresses the resilient modulus according to the bulk stress and the deviatoric stress, which allows us to take into account the effect of the shear behavior:

$$M_r = k_1 \left(\frac{\theta}{P_a} \right)^{k_2} \left(\frac{\sigma_d}{P_a} \right)^{k_3} \quad (1)$$

with,

$$\theta = (\sigma_1 + 2\sigma_3) = (\sigma_d + 3\sigma_3) = \text{bulk stress};$$

$$\sigma_d = \sigma_1 - \sigma_3 = \text{deviatoric stress};$$

k_1, k_2 and k_3 : model parameters.

For the Young modulus, the maximal values of the unconfined compression tests are chosen, by considering that the gravel lateritic soils are perfectly compacted in 95% of the Optimum Modified Proctor (OMP). For the asphalt layer and the subgrade (Young modulus (E) and Poisson's ratio (ν)), these values are chosen in reference to Fall, Senghor and Lakhoun (2002) [8]. The materials parameters are given in **Table 1**. The horizontal movements are blocked in the transverse directions (*flexible boundary*) and the vertical and horizontal movements are blocked in the bottom of the subgrade (*stiff boundary*).

For nonlinear analysis, an incremental iterative procedure is used, the tangent constitutive matrix is updated after and during each load increment (NCHRP, 2004). For this implementation, a direct incremental method of the resilient modulus with very small time steps is used. A first test showed that, for the linear method, 24 time-steps were sufficient to reach a constant result. Besides, for the nonlinear model, the tests showed that the

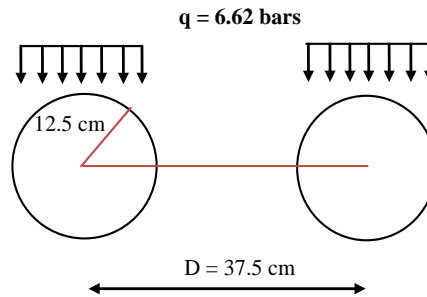


Figure 1. Schematization of the loading.

results vary very widely according to the compulsory number of steps. From 300 steps, the values stabilize, which explains that the value of the number of steps n was set to these aforesaid values. For every interval of load, the resilient modulus is given with the average of the values found for two successive stages. This algorithm is summarized in **Figure 2**.

Table 1. Characteristics of the axisymmetric linear and nonlinear models for the lateritic gravel soils of Ngoundiane (Samb, 2014 [3]).

Pavement layers	Thickness	Linear model		Nonlinear model		
	h_i (mm)	ν	E (MPa)	k_1 (kPa)	k_2	k_3
Asphalt	80	0.35	1.300	-	-	-
Base (<i>untreated</i>)	200	0.25	62	837.275	0.13	-0.33
Base 2%	200	0.25	84	279.074	0.65	-0.50
Base 3%	200	0.25	137	170.052	0.88	-0.56
Subbase (<i>untreated</i>)	250	0.25	62	837.276	0.13	-0.33
Subgrade	17.500	0.25	30	-	-	-

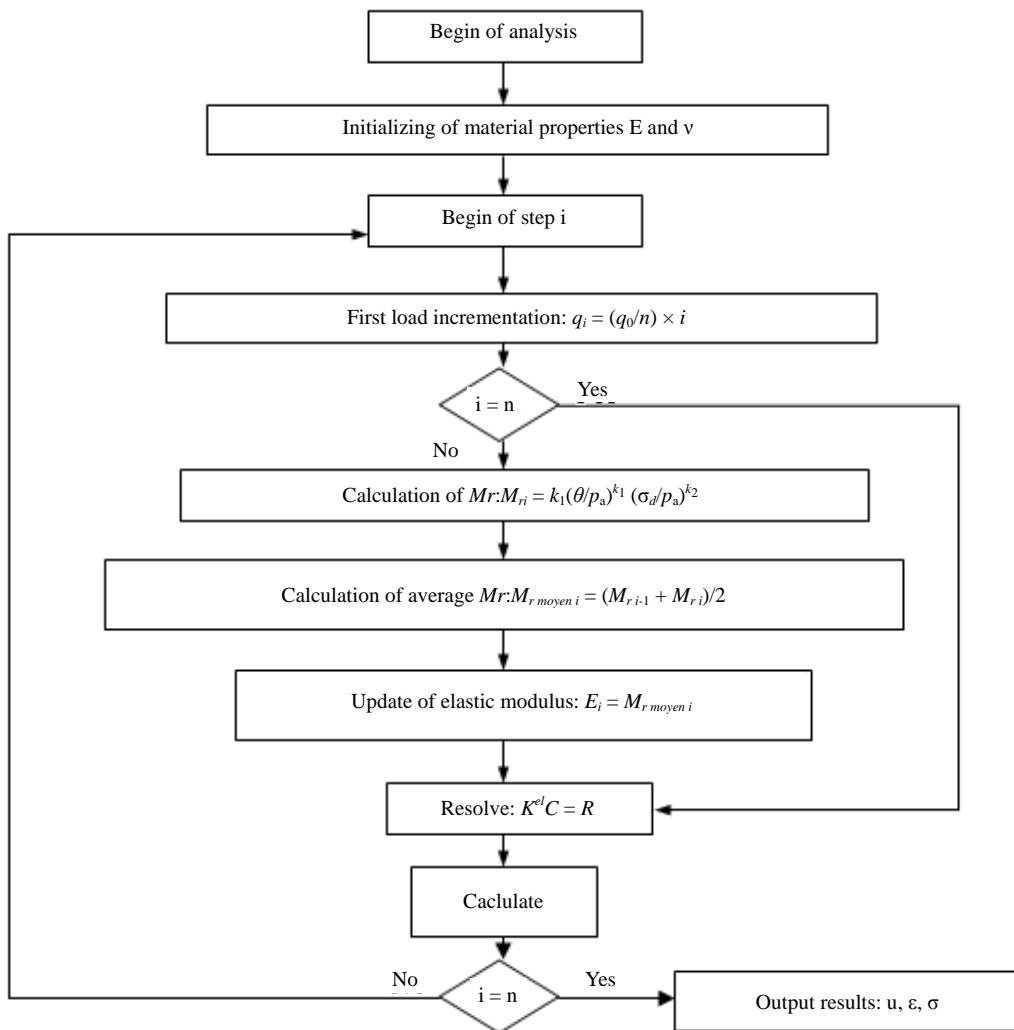


Figure 2. Calculation algorithm used in Cast3M[®] (Samb, 2014 [3]).

Impact of Overloading on the Deflection and the Vertical Strain of the Subgrade

The effect of overloading was studied with regard to the normalized axle load of calculation (13 tons). **Figure 3(a)** and **Figure 3(b)** and **Figure 4(a)** and **Figure 4(b)** give the variation of deflections and strains for the linear and nonlinear models. The results show a linear variation of the axle overload for both models. This proves that it is possible to know in advance the impact of the axle overload on deflections and strains of the pavement layers. We notice that the values of strains and deflections decrease according to the depth. Indeed, the values noticed at the subgrade are lower than those noticed for the other layers.

On the other hand, the impact of the axle overload seems to have more effect on deflection at the top layers (asphalt layer and base layer) than for the lower layers. It is necessary to note that the effect of a single wheel was tested. To know the total deflection and strain, it is necessary to take into account the effect of the dual-wheels. Besides, the variation of deflection and deformation for a variation of the axle overload of 1, 2, 3, 5 and 10 tons is given for the linear model (**Table 2**). These results show the possibilities of forecasting the response parameters values by analyzing loading scenarios. For a calculated estimation, **Table 3** gives a comparison of

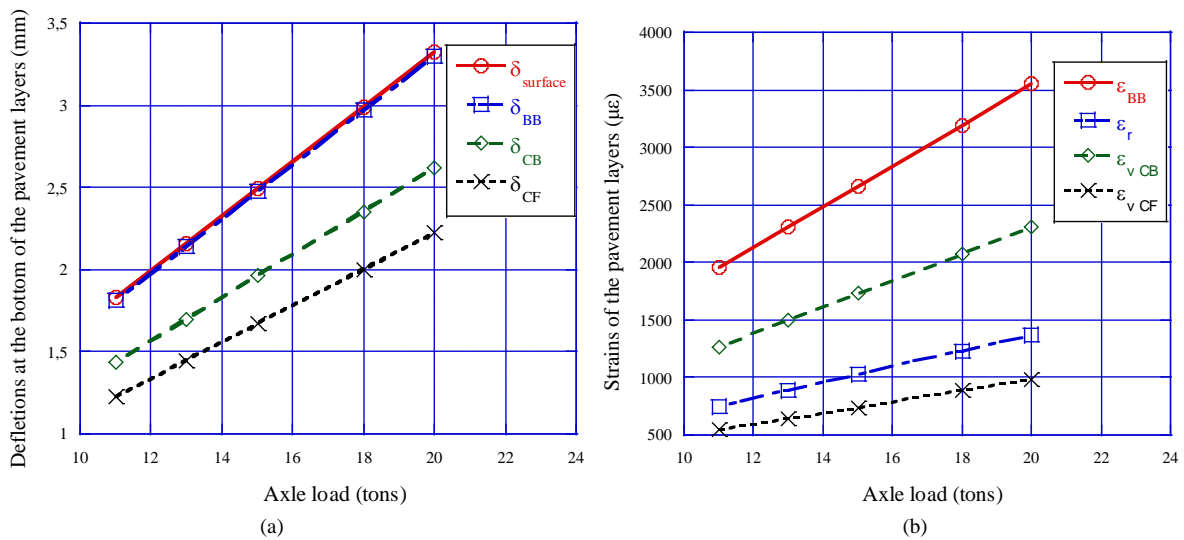


Figure 3. Variation of deflections and strains of the pavement layers (in absolute value) of the load for the 2D linear model: (a) Deflections; (b) Strains (Samb, 2014 [3]).

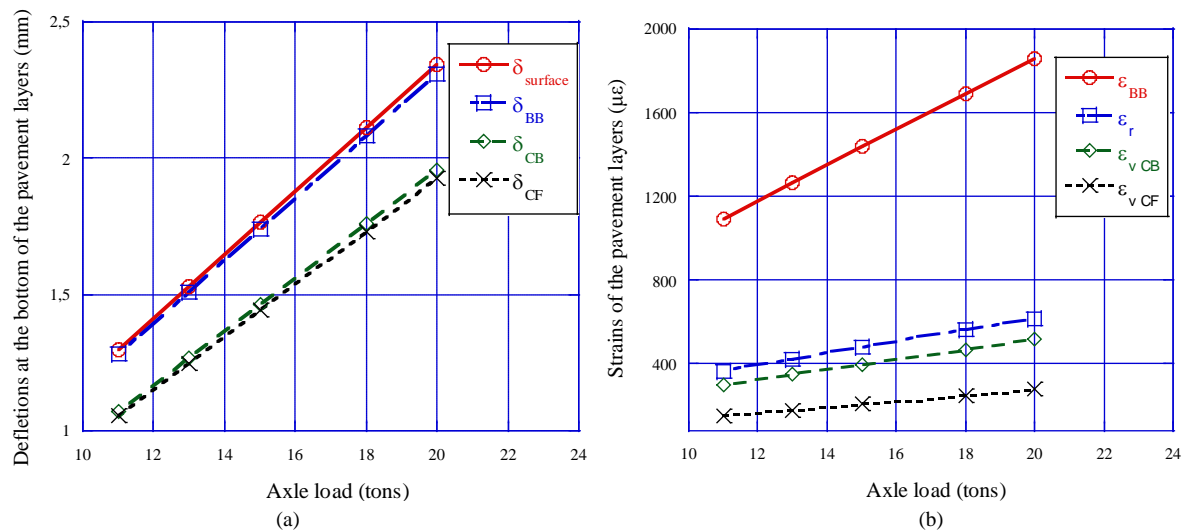


Figure 4. Variation of deflections and strains of the pavement layers (in absolute value) of the load for the 2D nonlinear model: (a) Deflections; (b) Strains (Samb, 2014 [3]).

Table 2. Deflections and deformations caused by the pressure of a tire by tons of axle overload for the linear model and for respectively: 2, 3, 5 and 10 tons (Samb, 2014 [3]).

	Deflections		Deflections according to the axle overload (mm)			
	Per tons (mm)		2 tons	3 tons	5 tons	10 tons
δ_{surface}	-0.04877		-0.09754	-0.14631	-0.24385	-0.4877
δ_{BB}	-0.04877		-0.09754	-0.14631	-0.24385	-0.4877
δ_{CB}	-0.0227465		-0.045493	-0.0682395	-0.1137325	-0.227465
δ_{CF}	-0.008193		-0.016386	-0.024579	-0.040965	-0.08193
	Deformations		Deformations according to the axle overload ($\mu\epsilon$)			
	Per tons ($\mu\epsilon$)		2 tons	3 tons	5 tons	10 tons
ϵ_{BB}	-137.42		-274.84	-412.26	-687.1	-1374.2
ϵ_r	56.0705		112.141	168.2115	280.3525	560.705
ϵ_{CB}	-81.526		-163.052	-244.578	-407.63	-815.26
ϵ_{CF}	-27.518		-55.036	-82.554	-137.59	-275.18

Notations: BB: asphalt layer; CB: base layer; CF: subbase layer.

Table 3. Variation of the critical response due to the pressure of a tire by tons of road overload (Samb, 2014 [3]).

	Variation per tons of overload	
	2D Linear	2D Nonlinear
δ_{surface} (mm)	-0.166	-0.116
δ_{BB} (mm)	-0.165	-0.115
δ_{CB} (mm)	-0.131	-0.098
δ_{CF} (mm)	-0.111	-0.097
ϵ_{vBB} ($\mu\epsilon$)	-177.370	-87.685
ϵ_r ($\mu\epsilon$)	68.291	28.778
ϵ_{vCB} ($\mu\epsilon$)	-115.200	-24.440
ϵ_{vCF} ($\mu\epsilon$)	-49.345	-14.245
σ_r (MPa)	0.065	0.019
σ_{CB} (MPa)	-0.008	-0.013
σ_{CF} (MPa)	-0.002	-0.001

the variation of deflections and strains for the linear and nonlinear models by tons of axle overload. We can thus notice that the linear model gives higher strain and deflection variations and lower stress variations than for the nonlinear model.

3. Conclusion

The results show a linear variation of deflections and deformations at the road layers according to the variation of the axle overload. This overload seems to have more effects on deflections for the top layers level (asphalt layer and base layer) than the lower layers. It is however necessary to note that the effect of a single wheel is tested. To know total deflections and deformations, it is necessary to take into account the dual tires. These results reveal the possibility of obtaining the response values of roads by analyzing real scenarios of load as well as forecasting the impact of the axle overload on deflections and deformations of road pavements.

References

- [1] UEMOA (2005) Règlement N°14/2005/CM/UEMOA relatif à l'harmonisation des normes et des procédures du contrôle du gabarit, du poids, et de la charge à l'essieu des véhicules lourds de transport de marchandises dans les états membres de l'Union Economique et Monétaire Ouest Africaine (UEMOA), 18-19.
- [2] BCEOM-CEBTP (1984) Guide Pratique de dimensionnement dans les pays tropicaux. Ministère Français de la Coopération, 155 p.
- [3] Samb, F. (2014) Modélisation par éléments finis des chaussées en graveleux latéritiques traités ou non et application au dimensionnement Mécanistique-Empirique. Thèse de Doctorat, Géotechnique, ED2DS, Université de Thiès, Thiès.
- [4] Lekarp, F., Isacson, U. and Dawson, A. (2000) State of the Art. I: Resilient Response of Unbound Aggregates. *Journal of Transportation Engineering*, **126**, 66-75. [http://dx.doi.org/10.1061/\(ASCE\)0733-947X\(2000\)126:1\(66\)](http://dx.doi.org/10.1061/(ASCE)0733-947X(2000)126:1(66))
- [5] Kim, M. (2007) Three-Dimensional Finite Element Analysis of Flexible Pavements Considering Non Linear Pavement Foundation Behavior. Dissertation, University of Illinois, Urbana.
- [6] Uzan, J. (1985) Characterization of Granular Material. Transportation Research Record No. 1022, Transportation Research Board, Washington DC, 52-59.
- [7] NCHRP (2004) Laboratory Determination of Resilient Modulus for Flexible Pavement Design. National Cooperative Highway Research Program (NCHRP) Project 1-28A. Transportation Research Board of National Academies.
- [8] Fall, M., Senghor, B. and Lakhouné, A. (2002) Analyse de la pratique du dimensionnement rationnel des structures de chaussée au Sénégal. Influence des paramètres d'entrée dans les codes de calcul pour le renforcement des chaussées. *Annales du Bâtiment et des Travaux Publics*, UCAD, FST, IST.

Field Scale Simulation Study of Miscible Water Alternating CO₂ Injection Process in Fractured Reservoirs

Mohammad Afkhami Karaei*, Ali Ahmadi, Hooman Fallah, Shahrokh Bahrami Kashkooli, Jahangir Talebi Bahmanbeglo

Department of Petroleum Engineering, Islamic Azad University, Firoozabad Branch, Firoozabad, Iran
Email: *mohammad.afkhami1@gmail.com

Received 13 October 2014; revised 13 November 2014; accepted 10 December 2014

Copyright © 2015 by authors and Scientific Research Publishing Inc.
This work is licensed under the Creative Commons Attribution International License (CC BY).
<http://creativecommons.org/licenses/by/4.0/>



Open Access

Abstract

Vast amounts of world oil reservoirs are in natural fractured reservoirs. There are different methods for increasing recovery from fractured reservoirs. Miscible injection of water alternating CO₂ is a good choice among EOR methods. In this method, water and CO₂ slugs are injected alternately in reservoir as miscible agent into reservoir. This paper studies water injection scenario and miscible injection of water and CO₂ in a two dimensional, inhomogeneous fractured reservoir. The results show that miscible water alternating CO₂ gas injection leads to 3.95% increase in final oil recovery and total water production decrease of 3.89% comparing to water injection scenario.

Keywords

Simulation Study, CO₂, Water Alternating Gas Injection, Fractured Reservoirs

1. Introduction

Miscible gas injection is one of the most important mechanisms of enhanced oil recovery from fractured reservoirs. Miscible gas injection may liberate and lead to production of a lot of amounts of oil that is entrapped into matrixes. Recovery from fracture-matrix system in laboratory scales started from 1970. Thompson and Mungan investigated results of laboratory experiments of gravity drainage in a fractured porous media under first contact miscible conditions. Basically, they compared replacement velocity with critical velocity and investigated its effect on oil recovery factor [1]-[5]. Water alternating gas injection is an effective method for controlling high mobility of gas in horizontal flooding which is used in so many reservoirs around the world and reported as

*Corresponding author.

successful operation. On the other hand, immiscible water alternating gas injection in oil reservoirs is not common [2]. Application of immiscible water alternating gas injection in USA is usually limited to onshore reservoirs. There are so many gas types with different characterizations used in miscible injection. Although many miscible gases include CO₂ and hydrocarbon gases, abundance of CO₂ and technical availability is an important parameter for improving miscible gas injection in USA [3]. Oil recovery factor using water alternating CO₂ gas injection is more than water injection, CO₂ injection, and hot CO₂ injection. Because of gas mobility, it penetrates into places which are unavailable during common injections [4].

Water flooding is an EOR method. One of the problems of water flooding is that the ions in water may be incompatible with reservoir fluid. It can lead to problems in ionic equilibrium which causes precipitation of heavy components of oil that can be a serious challenge in recovery from reservoir. Miscible water alternating CO₂ solves this inconvenience. Purpose of this study is to compare water injection and water alternative CO₂ gas injection and investigation of its effect on recovery factor and water cut from reservoir.

2. Interpreting Reservoir Model

Simulation of different phases in this project is done using a commercial software. Water flooding and water alternating CO₂ gas is tested in a two dimensional 1 × 25 × 25 grid block network.

A reservoir with all of no-flow boundaries are studied in this project. There are two phases of water and oil and no free gas. This model indicates a 200 acre (about 2950 ft × 2950 ft) reservoir. There is an injection well named INJ at the center of reservoir (at 13:13:1 grid block) and four production wells at the corners named P1, P2, P3, and P4. Production well P1 is at 1:1:1 grid block, P2 at 25:1:1, P3 at 1:25:1, and P4 is placed at 25:25:1.

Figure 1 depicts this reservoir from above. The wells are drilled with a 40 acre distance from each other and all of the wells started to production simultaneously. Depth from top surface of reservoir is 10,000 ft and reservoir net pay thickness is 50 ft.

Basic geological characteristics and different rock properties (porosity, absolute permeability, etc.) in each grid are specified at center of the grid block. Empty space volumes of blocks and inter-block transmissibility are calculated via simulator. The keywords used in this part depend on selected geometry option in initialization section. Cartesian, block-centered geometry option is used in this project. Porosity distribution is assumed to be homogeneous in reservoir and its value is 25%. But, permeability is inhomogeneous and has an average amount of 60 mD for the basic case. Original fluids in place including water and oil are saturated. Water occupies 20 percent of empty volumes and oil 80 percent. Residual oil and connate water are 15% and 20%, respectively. Initial pressure of reservoir is 4500.

As explained before, all the wells are drilled vertically. Inside diameter of wells are 0.5 ft and their depth is 10,050 ft and all the wells started production simultaneously (1st January 2010). All the wells produced for a period of 10 years with a constant 6 month controllers. There are 20 controller for each well in production period. Injection program has a controlled rate. Injected water rate is 3500 STB/day and injection rate of water alternating CO₂ is 3500 STB/day and 3000 Cuf/day, respectively. Production wells bottom-hole pressures are considered as constraints in water flooding. Minimum acceptable bottom-hole pressure is considered 2500 psi.

3. PVT Properties of Reservoir Fluids

Reservoir fluids are water and oil. The oil contains a constant and homogeneous saturation of dissolved gas with amount of 0.2 MSTB/day. Oil bubble pressure assumed 400 psi. Oil viscosity in base pressure of 4500 psi is 2.4 cp. Oil formation volume factor is 0.972. At the condition that water density assumed 2.4 lb/cuft, oil density would be 56 lb/cuft. Water compressibility assumed 3×10^{-6} psi⁻¹. At basic pressure of 4500 psi water formation volume factor assumed 1.0034 rb/stb and water viscosity assumed 0.96 cp. Rock compressibility assumed 1.4×10^{-6} psi⁻¹.

4. Water Injection and Miscible Water Alternating CO₂ Gas Injection Simulation

First, permeability distribution is depicted in **Figure 2**.

Cumulative oil production and water cut decrease during water flooding and miscible water alternating CO₂ gas flooding is shown in **Figure 3** and **Figure 4**, respectively. After miscible water alternating CO₂ gas injection, cumulative produced oil increases 3.95 percent and cumulative produced water decreases 3/89 percent.

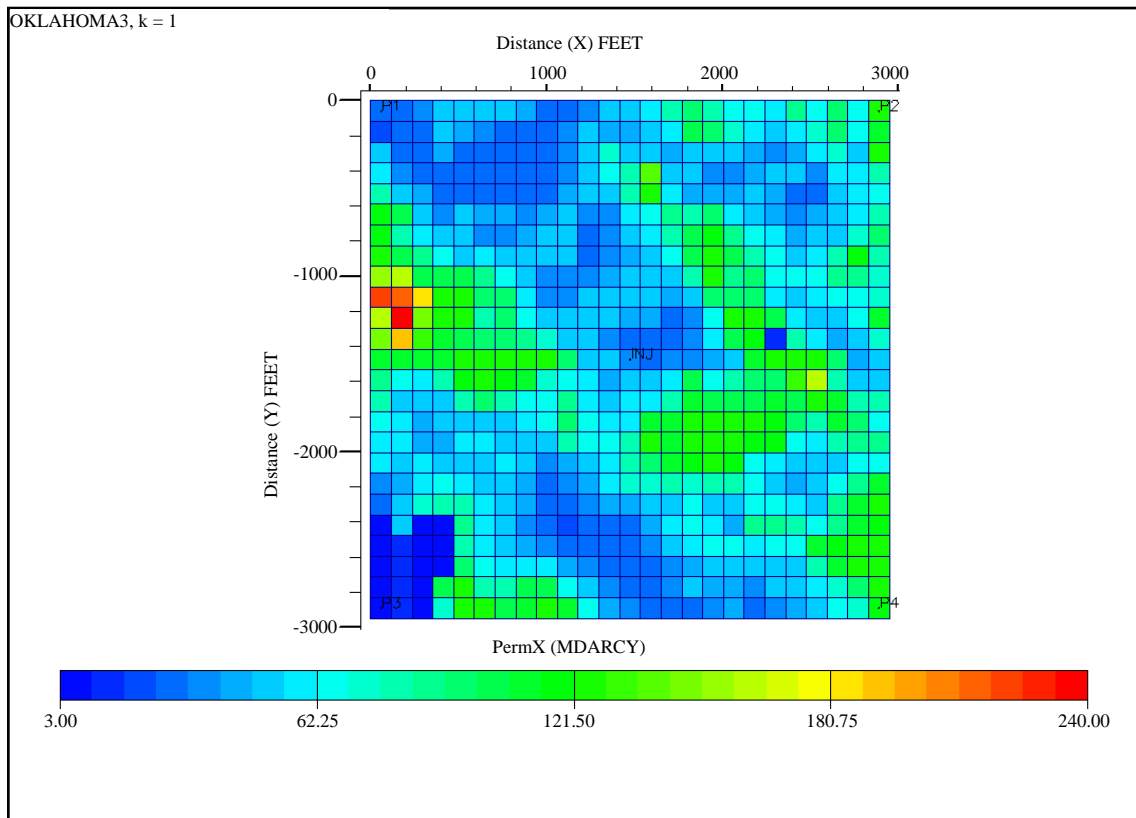


Figure 1. View of model from above that show permeability distribution in field and places of wells.

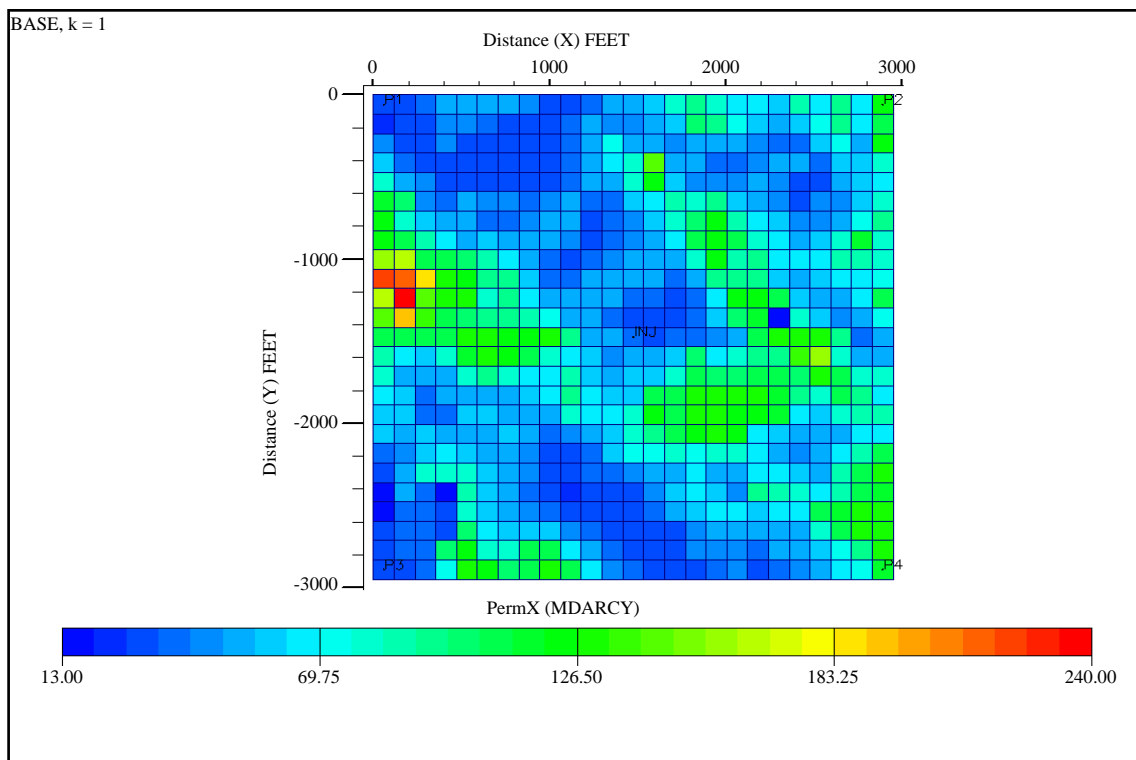


Figure 2. Assumed reservoir permeability distribution.

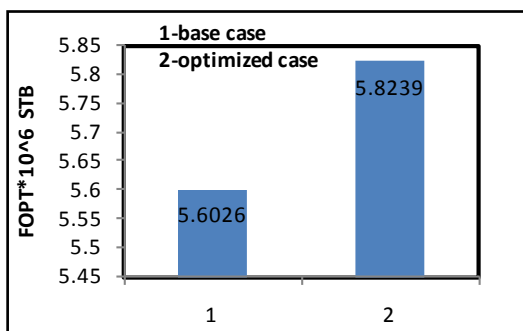


Figure 3. Cumulative produced oil in water flooding (1) and miscible water alternating CO₂ gas injection (2).

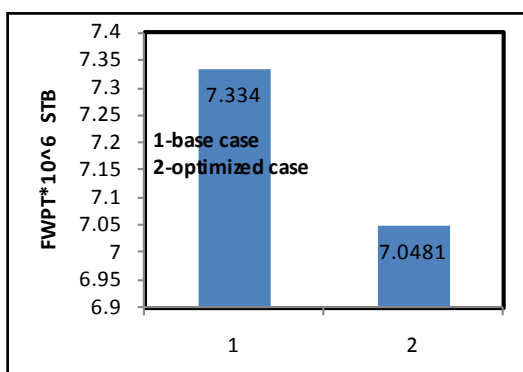


Figure 4. Cumulative produced water in water flooding (1) and miscible water alternating CO₂ gas injection (2).

Effect of miscible water alternating CO₂ gas injection on water saturation is shown in Figure 5 and Figure 6.

There is a noticeable change in water saturation distribution in all over the reservoir before the breakthrough. This can be seen in Figure 5 and Figure 6. Figure 5 shows water saturation distribution during water injection and Figure 6 shows water saturation distribution after miscible water alternating CO₂ gas injection. Via comparing Figure 5 and Figure 6 it is obvious that water saturation is more homogeneously distributed all thorough the reservoir in Figure 5. This means that sweeping efficiency increases after miscible water alternating CO₂ gas injection.

Figure 7 shows water cut for all the wells for water injection and Figure 8 shows water cut for all the wells in miscible water alternating CO₂ gas injection.

Water cuts of four wells are shown in Figure 7 and Figure 8 before and after miscible water alternating CO₂ gas injection. Via comparing Figure 7 and Figure 8 it is obvious that water breakthrough time and water cut curves almost tend to cover each other.

Water production rate curve for each production well during water flooding and miscible water alternating CO₂ gas injection also are shown in Figures 9-12.

By comparing above figures it can be seen that water production rate of production wells P1 and P3 increases after miscible water alternating CO₂ gas injection and water breakthrough happens earlier. It is because of bottom-hole pressure decrease of production wells P1 and P2 and oil production rate increase from these wells. Also, it is obvious that water production decreases from production wells P2 and P4 after miscible water alternating CO₂ gas injection and water breakthrough time is delayed. It is because of bottom-hole pressure increase of production well P2 and P4 and decrease in produced oils of these wells. Cumulative produced oil and water vs. time curves during water injection and miscible water alternating CO₂ gas injection are shown in Figure 13.

Cumulative produced oil and water plots are shown above. Via comparing these curves it is obvious that cumulative produced oil is increased after miscible water alternating CO₂ gas injection and cumulative produced water is decreased. In this project, cumulative produced oil is increased 3.95% and cumulative produced water is decreased 3.89%.

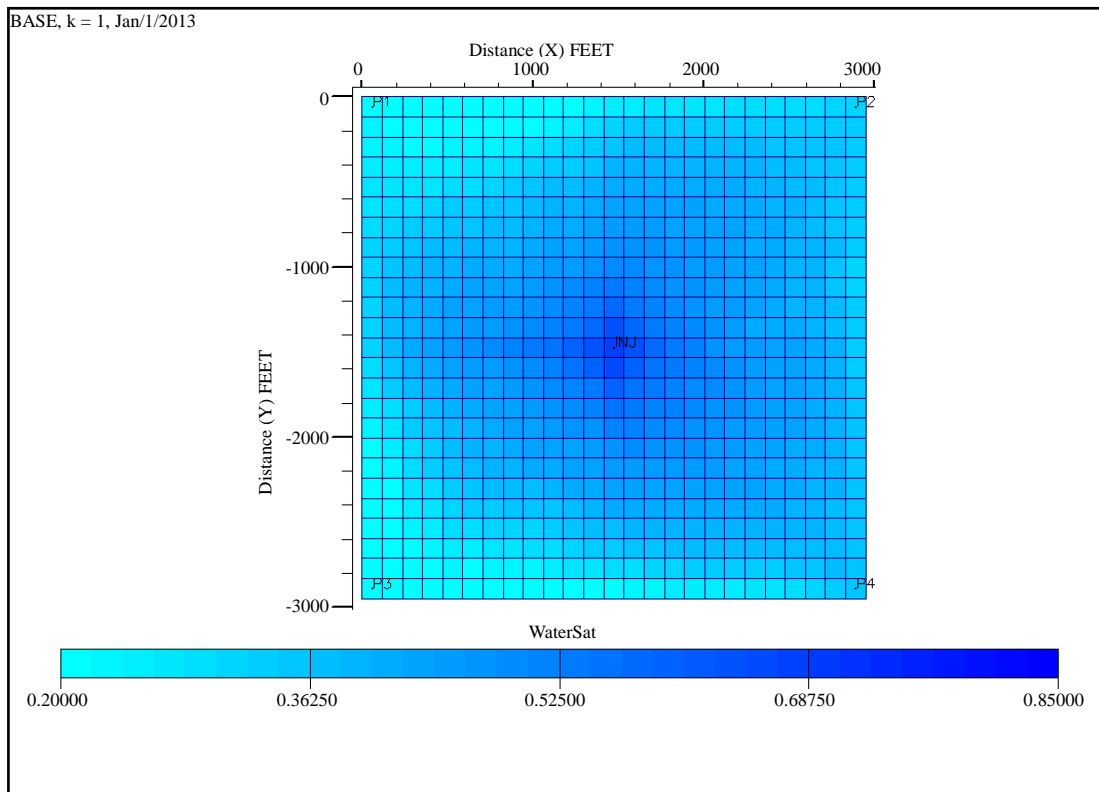


Figure 5. Water saturation distribution in water flooding.

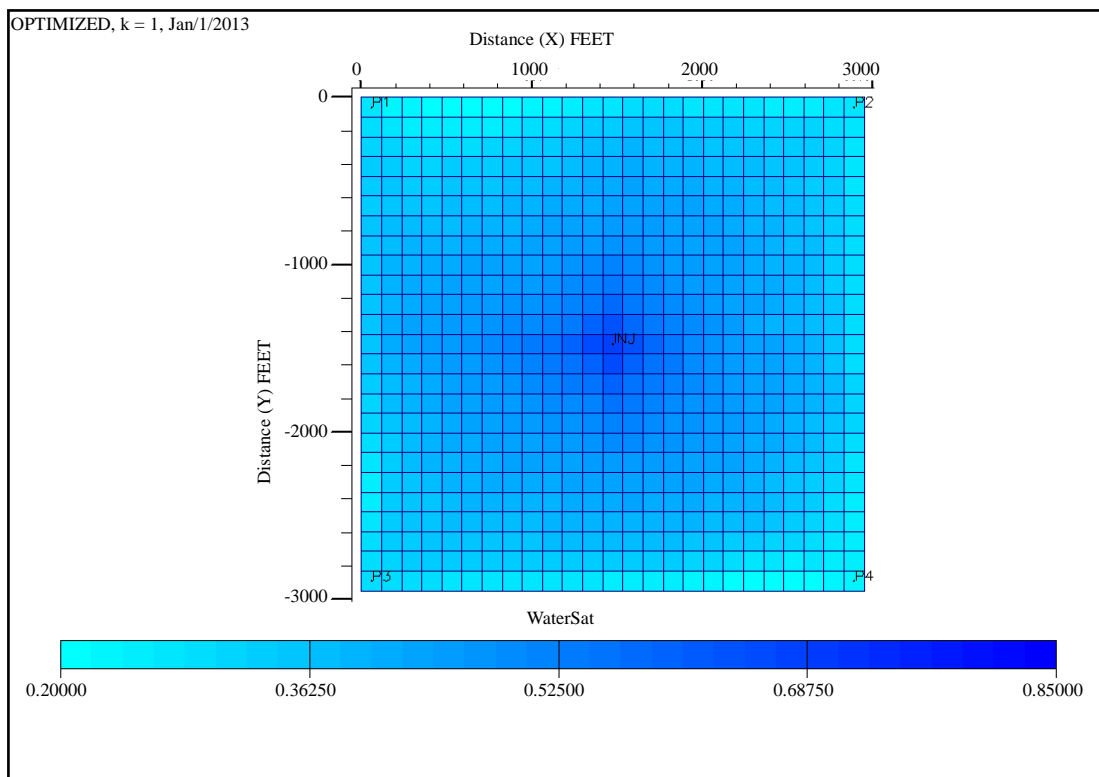


Figure 6. Water saturation distribution in miscible water alternating CO₂ gas injection.

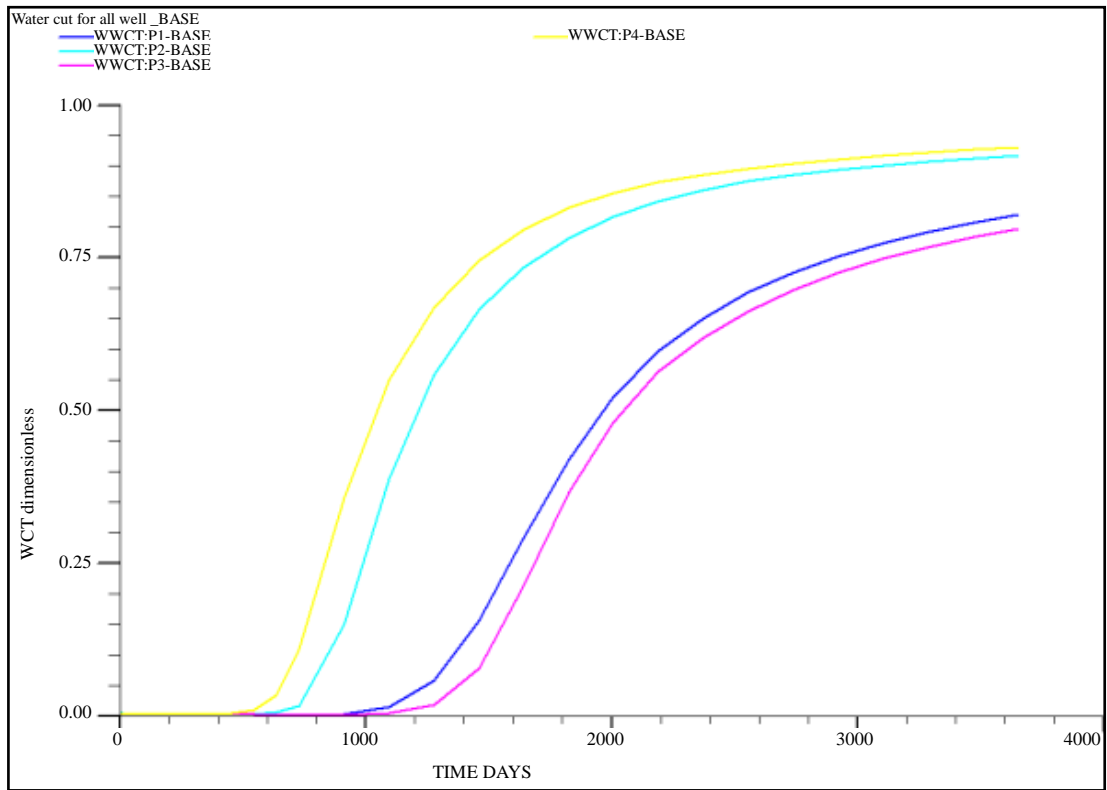


Figure 7. Water cut curves for all the wells during water injection.

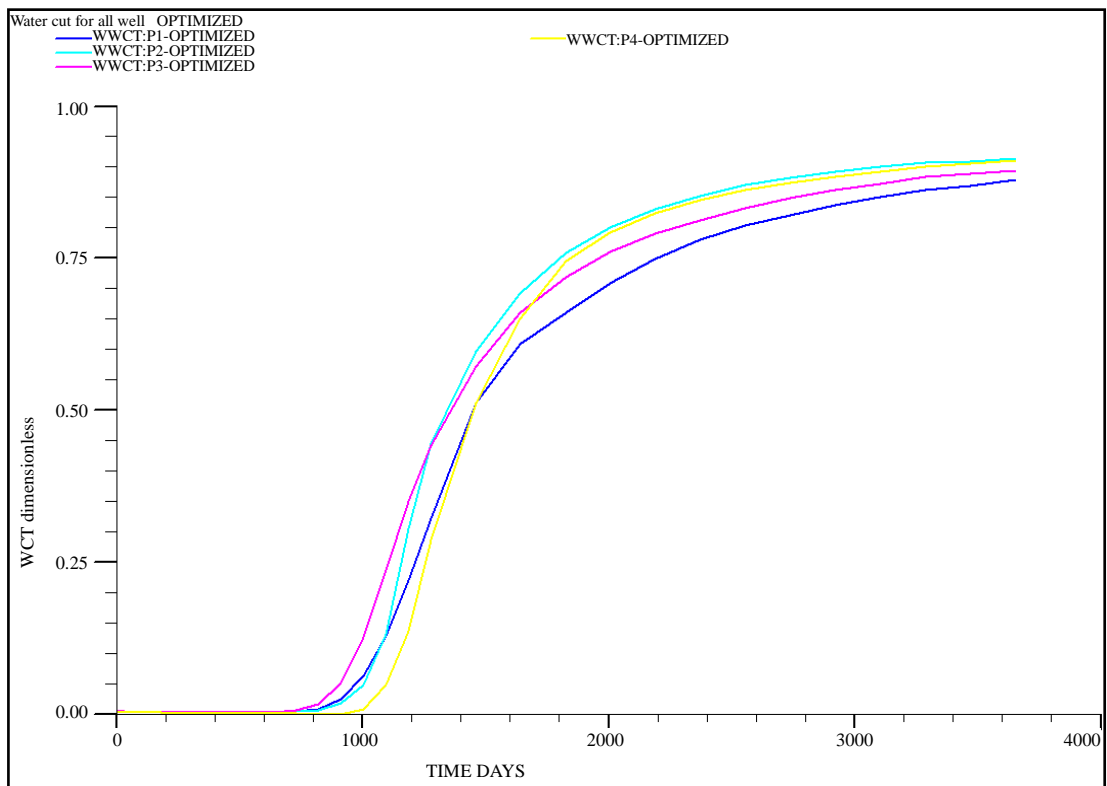


Figure 8. Water cut curves for all the wells during miscible water alternating CO₂ gas injection.

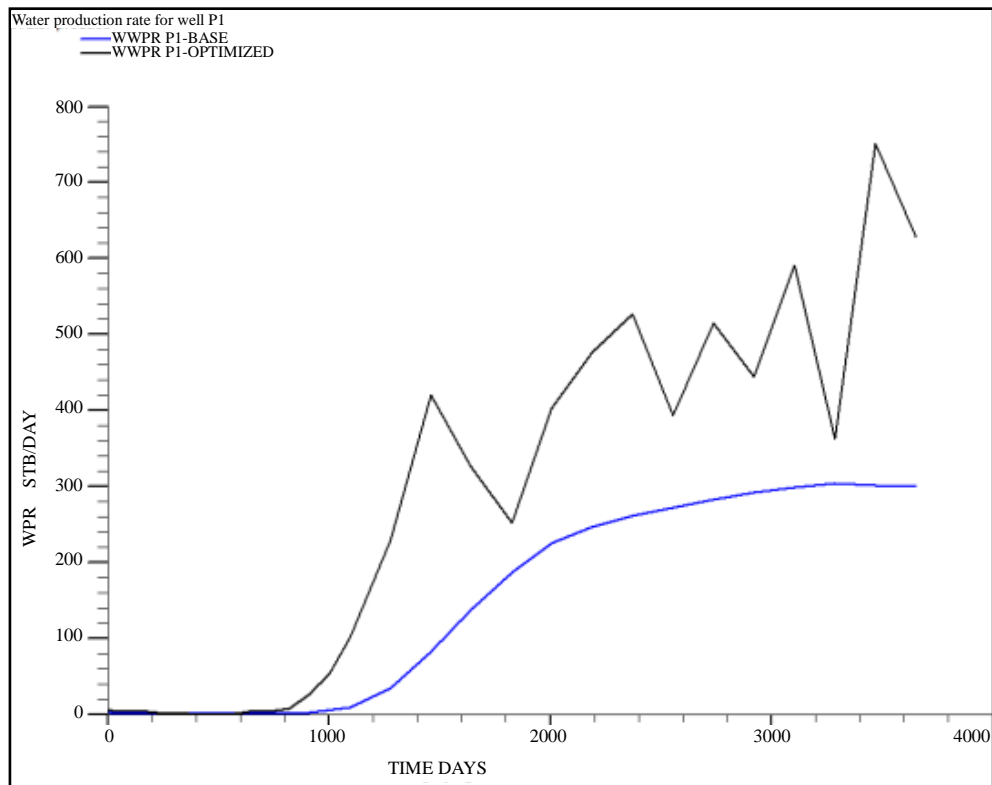


Figure 9. Water production rate from well P1 during water injection and miscible water alternating CO₂ gas injection.

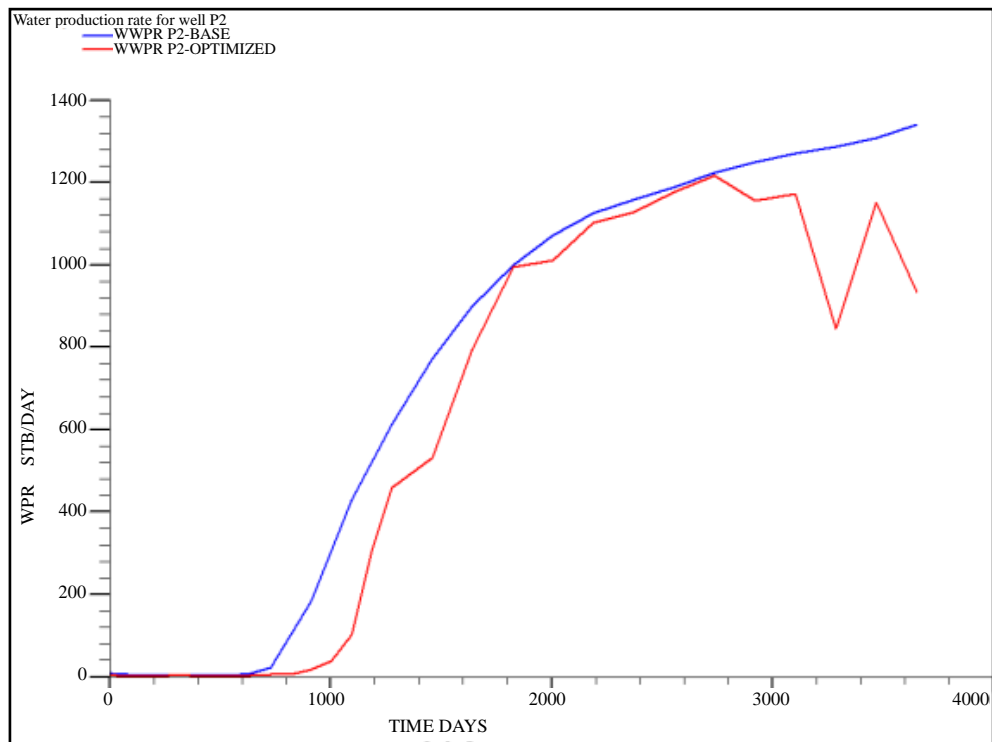


Figure 10. Water production rate from well P2 during water injection and miscible water alternating CO₂ gas injection.

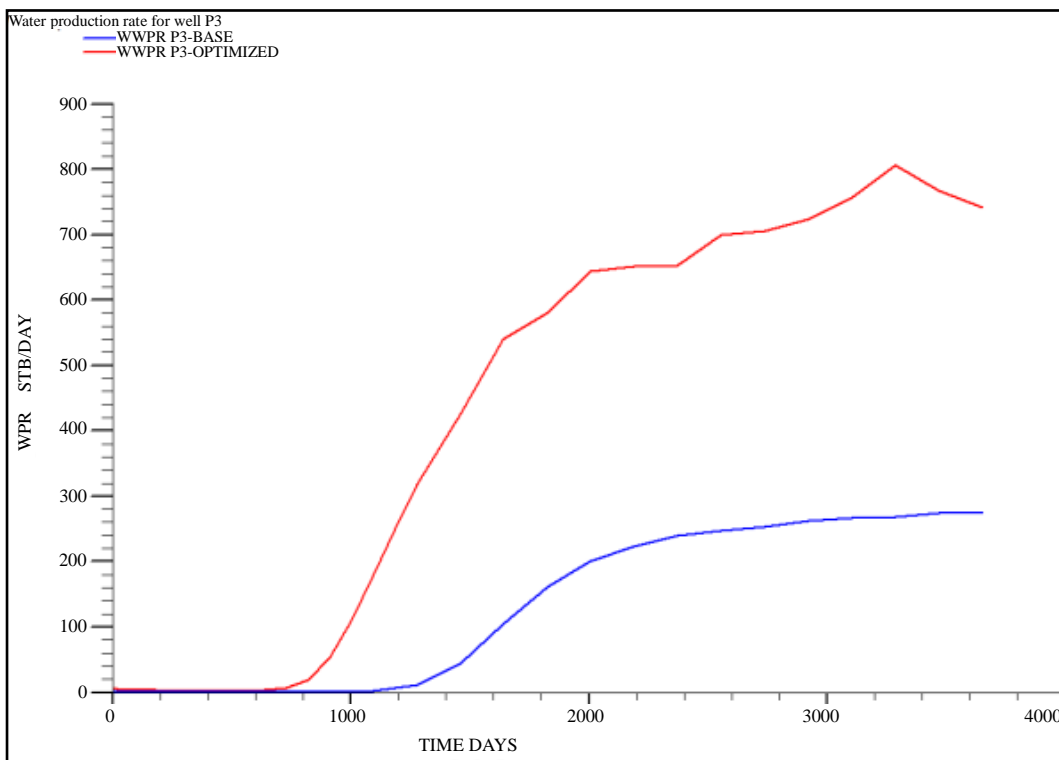


Figure 11. Water production rate from well P3 during water injection and miscible water alternating CO₂ gas injection.

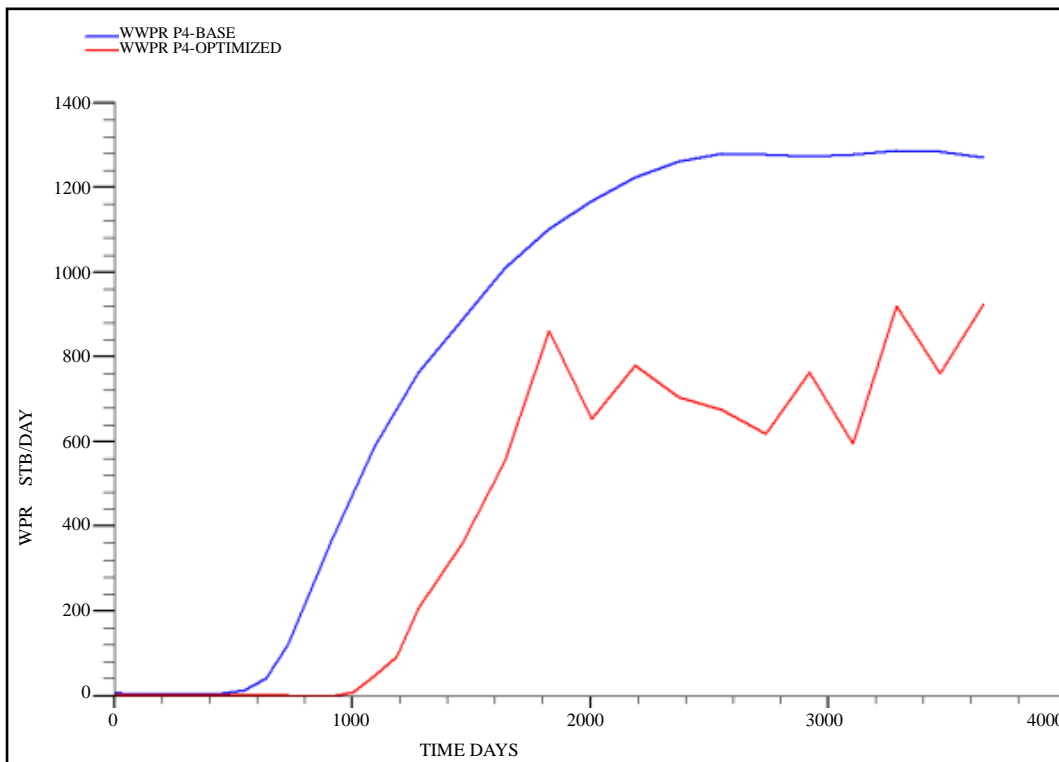


Figure 12. Water production rate from well P4 during water injection and miscible water alternating CO₂ gas injection.

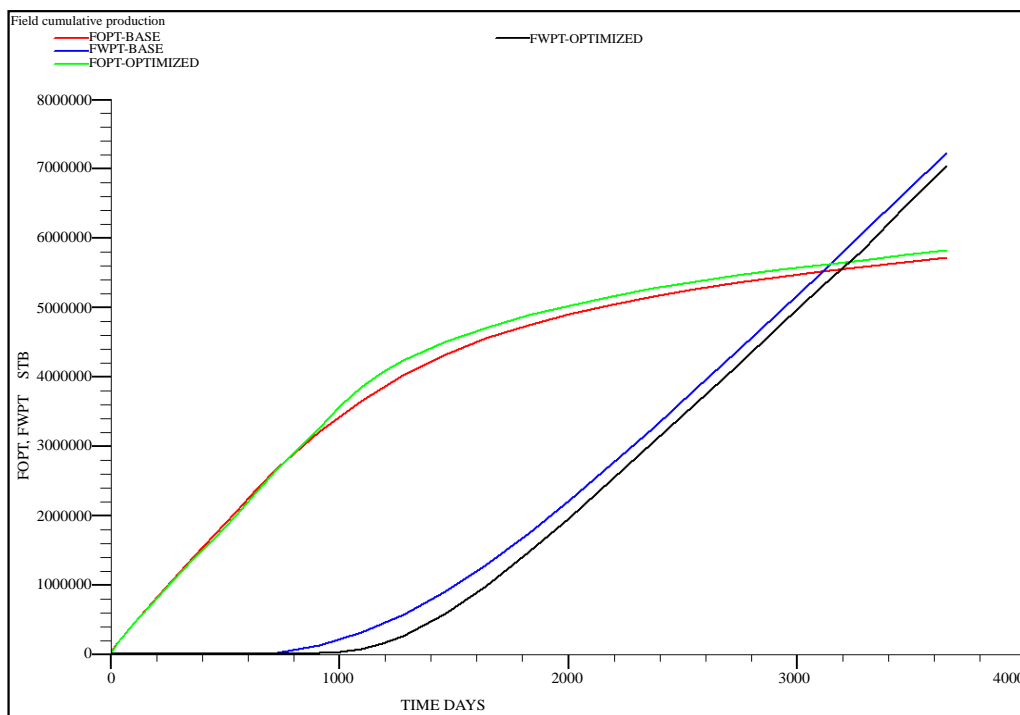


Figure 13. Cumulative produced oil and water during water injection and miscible water alternating CO₂ gas injection.

5. Conclusions

- Comparing water injection and miscible water alternating CO₂ gas injection, scenarios show that miscible water alternating CO₂ gas injection scenario has more efficiency comparing to water injection and produced oil and recovery factor would be greater in this method.
- Comparing water injection and miscible water alternating CO₂ gas injection, scenarios show that produced water during water miscible water alternating CO₂ gas injection scenario would be less comparing to water injection method.
- Water saturation during water injection scenario is more homogeneous all over the reservoir comparing to miscible water alternating CO₂ gas injection scenario. This would mean that sweep efficiency increases after miscible water alternating CO₂ gas injection.
- Most of Iranian oil reservoirs are fractured. So described method of miscible water alternate CO₂ injection is a suitable and recommended choice to be used in Iranian oil reservoirs.

References

- [1] Thompson, J.L. and Mungan, N. (1968) A Laboratory Study of Gravity Drainage in Fractured Systems under Miscible Condition. *The 43rd SPE Annual Fall Meeting*, Houston.
- [2] Christensen, J.R., Stenby, E.H. and Skauge, A. (2001) Review of WAG Field Experience. *SPE Reservoir Evaluation and Engineering*, **4**, 97. <http://dx.doi.org/10.2118/71203-PA>
- [3] Kulkarni, M.M. and Rao, D.N. (2005) Experimental Investigation of Miscible and Immiscible Water-Alternating-Gas (WAG) Process Performance. The Craft and Hawkins Department of Petroleum Engineering, Louisiana State University, Baton Rouge.
- [4] Dorostkar Mohammad, J. and Mohebi, A. (2009) Laboratory Evaluation of Warm Water Alternating Immiscible Gas Injection Warm of Carbon Dioxide for Enhanced Oil Recovery in Fractured Model. *Enhanced Oil Recovery—Iranian Chemical Engineering Journal*, **8**.
- [5] Taghavi, S.A. and Moradi, A. (2009) Compared Using Simulated Oil Recovery Factor of Miscible Gas Injection and Immisible Gas Injection in Iranian Fractured Reservoirs. *Enhanced Oil Recovery—Iranian Chemical Engineering Journal*, **8**.

Diagnosis Study of the Louga-Ouarack-Ndoyene R31 Regional Road (Senegal)

Seybatou Diop¹, Meissa Fall², Adama Dione², Moshood N. Tijani³

¹Institut des Sciences de la Terre, Faculté des Sciences et Techniques, Université Cheikh Anta Diop de Dakar, Dakar, Sénégal

²Laboratoire de Mécanique et Modélisation, UFR Sciences de l'Ingénieur, Université of Thiès, Thiès, Sénégal

³Department of Geology, University of Ibadan, Ibadan, Nigeria

Email: seybdiop@yahoo.fr, meissa.fall@univ-thies.sn, adama.dione@univ-thies.sn, tmoshood@yahoo.com

Received 20 December 2014; accepted 15 January 2015; published 19 January 2015

Copyright © 2015 by authors and Scientific Research Publishing Inc.

This work is licensed under the Creative Commons Attribution International License (CC BY).

<http://creativecommons.org/licenses/by/4.0/>



Open Access

Abstract

The degree of structural damage of the Louga-Ouarack-Ndoyene R31 regional road was surveyed using Lacroix deflectographe and geotechnical testing, in order to recommend possible rehabilitation measures aimed at maintaining the high level of service over the projected life span of the road. The data processing and interpretation were essentially based on the French standards and specifications, through which synthetic variables were generated with a qualitative significance and on the basis of which the extent of repairs and rehabilitation works to be undertaken were suggested. The decision grid thus produced, revealed road structure quality indices of mostly Q3, Q4, and Q5 types for a segment length of 36.954 km (equivalent to some 69.44% of the total road section), which justifies some major reinforcement works. The remaining part of the road section (nearly 30.56% with road quality indices \leq Q2) is still in acceptable condition, requiring only some minor maintenance works. The rehabilitation costs were estimated to be of the order of 5,352,000,000 (five billion three hundred fifty-two million) CFA francs, based on local market price conditions.

Keywords

Senegal, Road Diagnosis, Lacroix Deflectograph, Deflection, Reinforcement, Maintenance

1. Introduction

As part of the mission of regular follow-up of the Senegalese' network of "classified roads' system", the

SENELABO-BTP laboratory conducted a diagnostic study of the R31 regional road, on behalf of AGEROUTE-Senegal (Agence des Travaux et de Gestion des Routes du Sénégal). The goal was to identify renovation/rehabilitation works required in order to maintain the level of service after the projected lifetime of over 10 years.

For this study, three complementary indicators to provide assessment on the road edifice were analyzed: 1) its structural behavior (viz., the deformability of the road under the effect of a rolling load); 2) the appearance of the road surface characteristic (apparent pavement damages); and 3) the geotechnical properties of the constituent materials of the various layers of the road. The focus of this paper is to present the methodological approach and the investigations results, the outcome of which can be of advantage to the Senegalese Road Administration as new tools in road diagnosis techniques.

2. Materials and Methods

2.1. Materials

Site description and road structure: **Figure 1** is a lay-out plan showing the study road R31. Out of a length of about 53.500 km, the R31 regional road supports a T2 traffic type (viz., a traffic type with up to 1000 vehicles/day). It was built in 1998 with the key mission of serving the traffic of people and goods, and for the transport of merchandises from the rural economy within the regional administration of Louga; a district that accounts for approximately 678,000 inhabitants and covers an area of about 29,200 km².

In terms of geomorphology, this area is characterized by the extension of relatively flat and open landscapes of sand dune systems (quaternary ergs). The climatic conditions are typically Sahelian, with nearly 70% of the

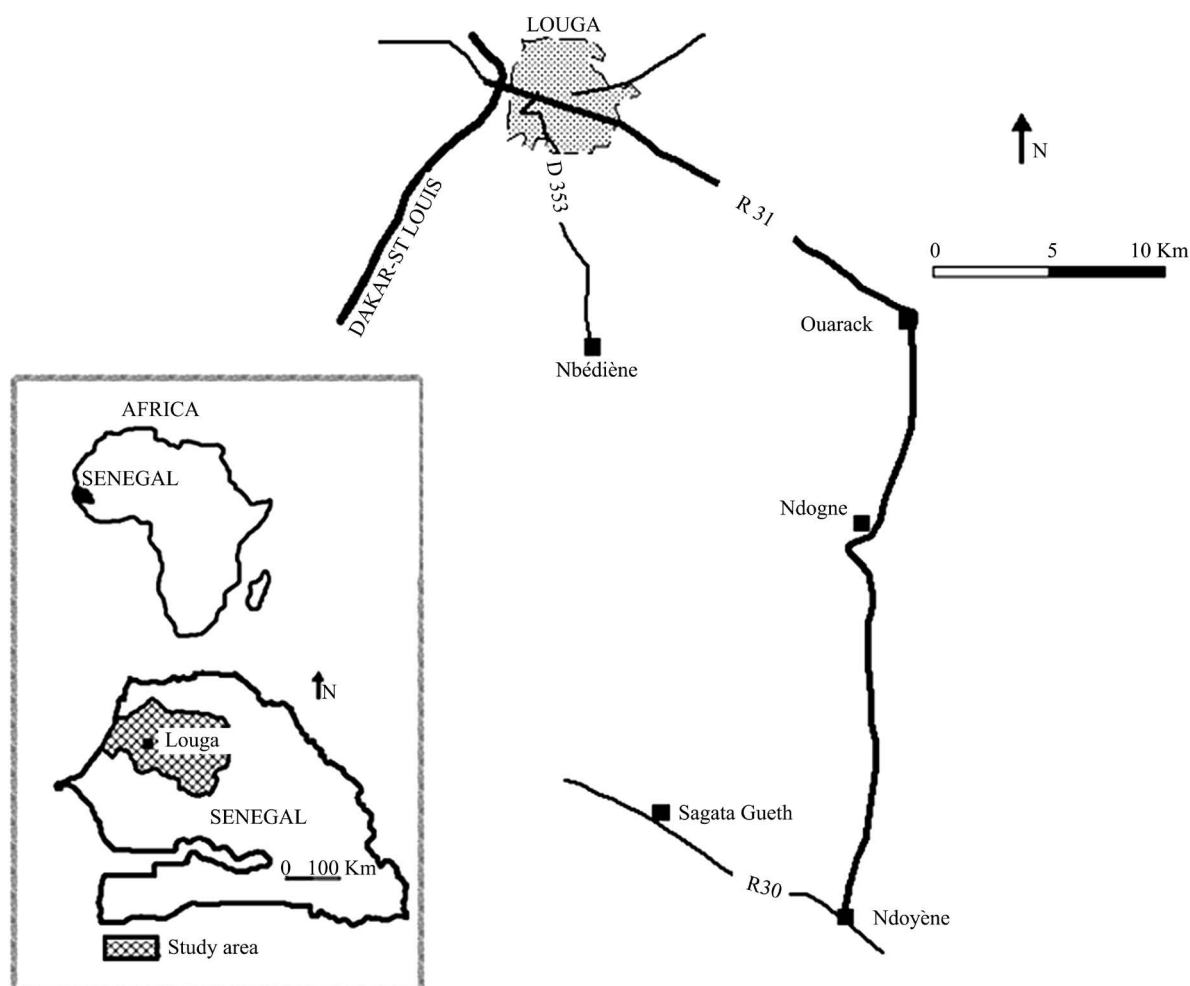


Figure 1. Location map of the study road.

annual precipitation occurring between the months of July and September. The average annual rainfall places the region between the isohyets 300 - 400 mm, which implies a savanna vegetation system. The land use is mainly for the cultivation of groundnuts and millet; but truck and cattle ranching are also important in the area.

The studied road comprises of a 5 cm thick layer of asphalt (bituminous pavement), a base layer of 20 cm lateritic gravel stabilized with cement, a 35 cm thick foundation (sub-base) layer (clayey sands) and a 40 cm thick subgrade of sand resting on the sandy original grounds (**Table 1**).

2.2. Methods

The data bank available for the investigations comprised of measurements of the deformability of the pavement structure using the type O2 Lacroix deflectograph (LD) (**Figure 2(a)**). These data were complemented with other available information such as data from auger holes drilling by hand and mechanical shovel at different PKs, and from the retrieved samples, and data from the VIZIR campaign conducted in May 2012 by the APAVE Sahel company in order to assess the severity of pavement degradations.

The campaign of deflectometric measurements was carried out by SENELABO-BTP Company in December 2012 immediately after the rainy season, which corresponds to the period of the year when water content in the subgrade is high. The bearing capacity of the road layers is minimal at this time period, as compared to the relatively higher values during the dry period. At the moment there are no experimental data in Senegal to be employed for possible seasonal data corrections in relation to the period of measurement. In addition, geotechnical surveys were also conducted in October 2012 by the company SENELABO-BTP. A series of samples were collected at 10 km interval, beginning from PK 0 (Louga town). The identification tests on sampled materials were performed in the laboratory based on standard tests such as grain size distribution [1]; soils classification [2]; oedometer methods [3]; methylene blue test [4]; CBR test [5]; modified proctor test [6]; water content determination [7].

Data processing was performed based on the standards and technical specifications developed from the results of methodological research in recent years ([8]-[13]) and used as recommendations and decision tools in terms of diagnosis and estimation of the 'refection' works to keep safety. This enabled us to achieve a good description of the structural conditions of the road, and establish the section to be repaired, as well as the nature of the most realistic rehabilitation measures to be undertaken.

Principle of the Lacroix deflectograph. Mounted on a truck, the Lacroix deflectograph (LD) allowed for quick survey of the pavement structure and coverage of more points per unit time compared to the famous Benkelman beam. Its technical characteristics are presented in **Table 2**. The LD allows the measurements of the deflection basin (deflection bowl) generated by a passing truck. The instrumental device includes an automatic pilot system of data acquisition, control and processing. The vehicle running at a constant speed (between about 2 - 4 km/h), thus simulates a passing heavy-weight-truck (axle load ~13.2 tons), traveling approximately at 70 km/h and records at the same time the deformation induced on the road structure (deflection basin; **Figure 2(c)**) using several sensors (two arrays of geophones distributed along a beam) that records transversal surface profiles. The goal is to measure in real magnitude the response/deformation of the road structure (viz., the bearing capacity of the subgrade and stiffness of the road pavement and thus evaluate its ability to withstand a heavy traffic load). The deflection/deformation is assumed to vary with the stiffness of the road.

Figure 2(b) schematizes the measurement principle of the LD. The operating procedure involved: first, placing of the measuring beam on the surface of the pavement, along the wheel paths between the wheel axles. The vehicle then drives at a steady speed. The measuring beam under the vehicle remains fixed until the rear axle exceeds 10 cm of the point of measurement. The stress related to the passage of the vehicle causes a deformation

Table 1. Structure cross section of the study road.

Depth (m)	Layer	Composition
0.00 - 0.05	Surface course	Asphalt concrete
0.05 - 0.25	Base	Cement treated lateritic gravels
0.25 - 0.60	Foundation	Clayey sand
0.60 - 1.00	Subgrade (platform)	Sands (natural terrains)

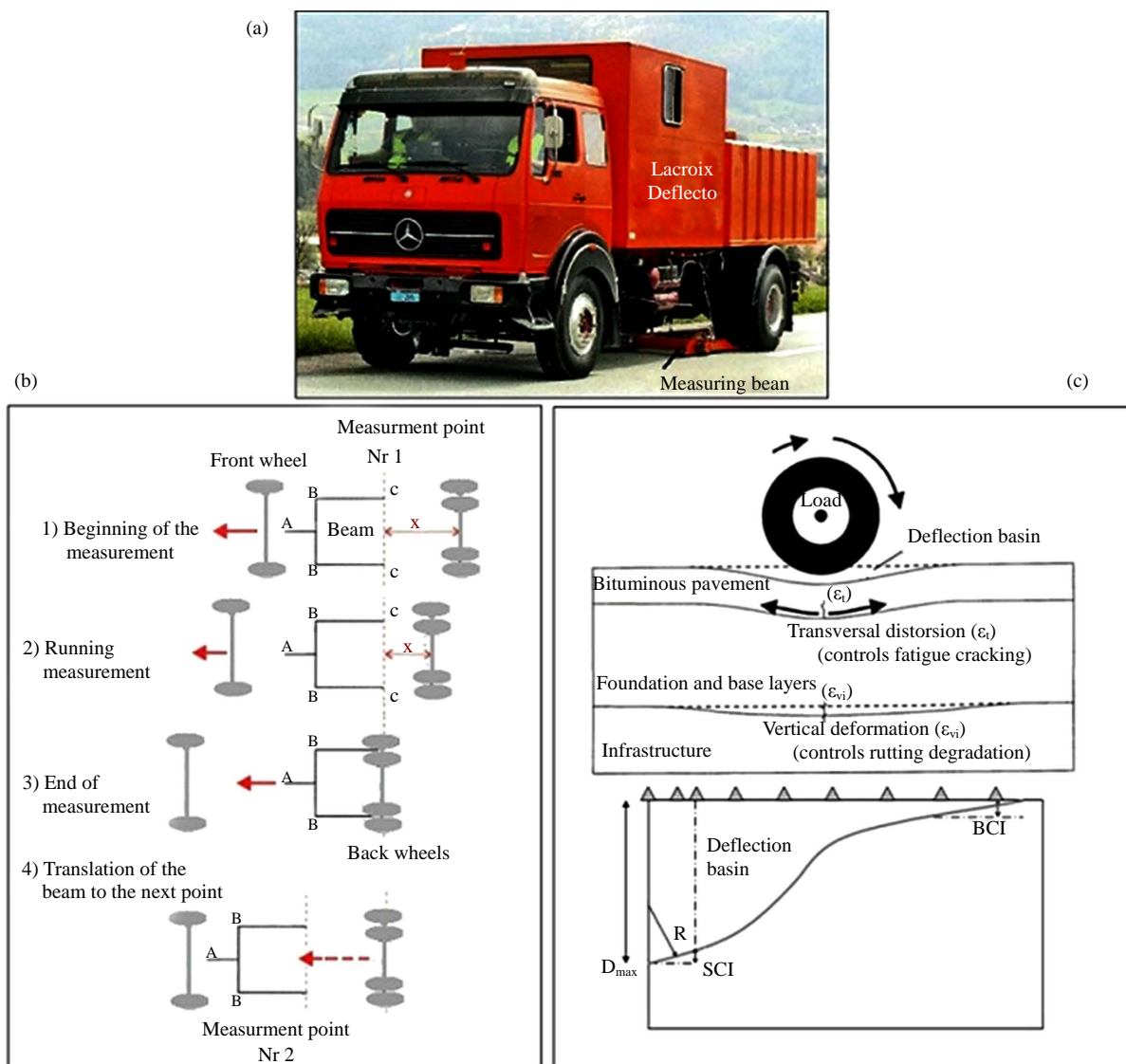


Figure 2. The Lacroix deflectograph: (a) Measurement frame; (b) Measurement principle; (c) Deflection basin and main parameters. (D_{max} is the deflection under the rolling load; R is the radius of the deflection basin; ϵ_{vi} is the vertical deformation in the subgrade; ϵ_t is the transversal deformation in the asphalt concrete (pavement) layer; SCI is the index of surface curvature and BCI represents the index of base curvature) (modified after [14].)

Table 2. Main characteristics of the type 02 LD (modified after [14]).

Constructor	CECP angrers
Type of carrier vehicle	GLR 260
Type of electronic device	LEEM
Method of load application	Rolling wheel load
Speed of applied load	10 km/h (5 Hz)
Vehicle speed	2 - 4 km/h
Measuring step	4 - 6 m interval
Sensor resolution	1/100 mm
Location of measures	On the wheel paths between the wheel axles
Measure within the deflection basin	65 points (flexible pavement)
Applied load level	Axles weight ~13.2 tons
Probed superstructures types	Flexible and semi-rigid pavements (stabilized foundation)

on the road floor which is recorded by the sensors (Figure 2(c)). The deflection basin thus created by the passage of the vehicle is subjected to 65 points of measurement before the system moves forwards over 4 - 6 meters to the next measuring station by pulling the measuring beam. Further details on the measurement principles and procedures are presented elsewhere in cited reference standards and literature (e.g., LPC No. 39 [4]).

However, it should be noted that the resulting data from a LD measurement campaign can be used for various investigation activities and design of pavement structure ([15]-[19]), particularly in the analysis of deflections as indicators of performance (diagnosis and control) as well as in “back-calculations” of the ground E-modules to evaluate the residual modules of the road’s component layers and to optimize the prediction for the reinforcement of a pavement structure. There are formulae linking the value of the measured deflection to related “efforts” in the layers and thereby allowing the determination of the structural conditions and critical parameters responsible for the road degradation in terms of ageing and deformation of the pavement at the location of measurement (see Figure 2(c)).

3. Results and Discussion

3.1. Measure of the Road Deformability

Data from the measurements carried out with the LD road deflection tester were evaluated with the help of the WLFX 32 software (version 6.1.0). The procedure includes: 1) reading the charts records (deflection profiles); 2) conversion into numerical values, after calibration of the sensors, which will allowed for reading the measurements with a precision of 1/100th mm; 3) calculating the average value of the maximal deformations/deflections (Md) recorded within the deflection basin, and the standard deviation (σ) in order to highlight any (possible) heterogeneity within the deflection basin.

In this study, the deflection basin was referred to as a “homogeneous” deformation, if the value of σ is $\leq 15 \times 1/100$ mm; and “heterogeneous” when the value of σ is $> 15 \times 1/100$ mm. On the assumption of “homogenous” deformation within the basin, the so-called “characteristic deflection” (Cd) of the investigated zone can be defined using Equation (1), the numerical value of which provides guidance on the mechanical behavior of the floor structure and allows for appreciation or diagnosis of the state of the pavement structure at the measurement point (Table 3 and Table 4).

The degree of deformation with respect to passing load depends on the type of road surface (flexible or semi-rigid). For a fully flexible road it was established [20], that there is a relation between the degree of structural damage, the measured Cd-value and the traffic load that have already passed on the road. Under certain conditions the ground modulus (Es) can be estimated based on the Cd-value and the equivalent thickness of the road structure [14]. Cd values can be used to assess the remaining service life of a road floor or to dimension it with respect to the allowable deflection. In this study, the Cd value of a monitored zone was estimated graphically from the Md-value (average deflection), using the following statistical relationship (Equation (1)). That is to say, by assuming a probability level of exceeding the Md value of 10%.

Table 3. Correlation between the parameters Cd, bearing capacity and quality level of a road structure (modified after [3]).

	Cd values (1/100 mm)		
	Cd1 = 60		Cd2 = 80
Qualitative appréciation of Cd	Low	Medium	High
Bearing capacity of the road edifice	High	Poor	Low
Quality level of the road edifice	Good	Doubfull	Bad

Table 4. Interval class values for the characteristic deflection [18].

Deflections class	C1	C2	C3	C4	C5	C6
Cd value ($\times 1/100$ mm)	0 - 49	50 - 74	75 - 99	100 - 149	150 - 199	200 - 300
Level of deflexion	Low		Medium		High	Very high

$$Cd = Md + 1.2826 \frac{\sigma}{\sqrt{n}} \quad (1)$$

Threshold for critical deflections. The procedure of data analysis required establishing “threshold” values as a qualitative basis for appreciating the measured values. **Table 3** shows the parameters considered in the process of qualitative data analysis of the road structure in terms of threshold values for the characteristic deflections.

Due to lack of reference value or standard for the Senegalese road network system, the critical threshold values were defined with reference to the “Handbook for Building Flexible Pavements in Tropical Countries” [3].

Thus the following values were adopted in this study (**Table 3**): $Cd1 = 60 \times 1/100$ th mm (threshold value below which the structure behaves satisfactorily) and $Cd2 = 1/100 \times 80$ mm (threshold value above which the structure has bearing defects). These limits normally characterize the road structures for which constituent materials have been emplaced mechanically. The numerical values may vary in principle according to the geographical location and the local climatic conditions, and are normally derived from an experimental validation procedure based on a series of LD measurements’ campaigns in the area of interest.

It is worth noting at this stage of the discussion that the measurement campaigns resulted in a large data set. The data were then processed in a multistep procedure which allowed for division of the monitored road into some 170 separate sections or segments regarded as homogeneous zones. Each homogeneous zone is regarded as a zone where the maximal deflection does not vary significantly (standard deviation $\sigma \leq 15 \times 1/100$ mm); in other words, within a homogeneous zone the pavement responds in a similar way to the applied load. Consequently, the decision to take a particular action is based separately on the individual homogeneous zone. For convenience, however, the monitored road section need not be divided into relatively short zones [20], so the minimum length can be set for the survey. In this study a minimum length of 50 m was arbitrarily adopted for the zones. The large number of the individual zones implied the use of the graphical dual axis mode of representation (**Figure 3** and **Figure 4**) for the parameter values.

Classes of Cd values. These were defined based on **Table 4**. The distribution pattern (**Figure 3**) shows a high variability of the values, although suggesting a predominance of the low deflection levels ($Cd \leq 60 \times 1/100$ th mm). Since the road has been initially designed to support a T2 traffic class and still exhibits a S3 bearing capacity platform class ($15 \leq CBR \leq 30$; see **Table 6**), the levels of deflection could be classified as weak to moderate on the most part of the road section length. This would mean a road structure of *good to doubtful* quality on the road sections. Further discussion on this will be presented later in the subsequent section below.

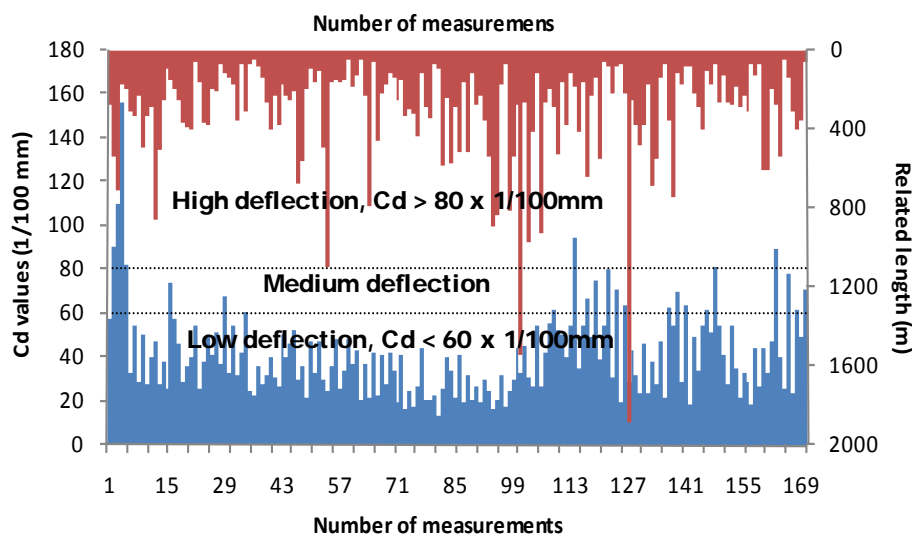


Figure 3. Histogram of section lengths surveyed and their corresponding Cd values. Note the following features of the graph: range of Cd values $< 60 \text{ mm} \times 1/100$: low deflection (elevated residual bearing capacity, the road edifice is still good); values range $60 \times 1/100 \text{ mm} \leq Cd \leq 80 \times 1/100 \text{ mm}$: medium deflection (poor residual bearing capacity, the structure of the road edifice is doubtful); Cd values $> 80 \times 1/100 \text{ mm}$: high deflection (low residual bearing capacity, the road edifice is bad).

3.2. Pavement Damages

The results of classifying the apparent pavement damages using the index values (I_s) derived from the VIZIR study [21] are graphically presented in Figure 4, while the results were also categorized based on Table 5 [22], after some corrections taking into account the recent cosmetic reparation works on the study road. The I_s value was calculated by combining the cracking index (I_f) (*i.e.* degradation couple: cracking/crazing) with the deformation index (I_d) (*i.e.* degradation couple: deformation/rutting). As shown by the graphic presentation, zones with degradation indices greater than 3 ($I_s > 3$) occur more frequently suggesting that many zones of the road section exhibit large surface structural damages. Consequently, their degradation's level can be characterized as medium to bad which ultimately require that rehabilitation works should be undertaken.

3.3. Geotechnical Properties of the Road Layers' Constituent Materials

The results of the laboratory investigations as presented in Table 6 revealed the following facts: 1) The platform (subgrade) is essentially a sand gravel, with a small non-swelling fine fraction of medium plasticity index; whereas materials of the foundation layer (sub-base) are made of clayey sands; 2) The bearing capacity of the subgrade is in the S3 class ($15 \leq CBR \leq 30$) over the entire road section, which means it is still suitable. In contrast, the bearing ratio of the sub-base materials ($CBR \approx 18$) appeared low, and far below the technical specifications of $30 \leq CBR \leq 60$. In addition, with CBR indices in the order 55 to 60, the materials of the base layer (lateritic gravels improved with cement) show some severe bearing defects, compared to the requirements of the technical specifications of CBR range of ≥ 80 for raw materials and CBR of ≥ 160 for materials treated with cement.

In summary, the sub-base still kept a proper bearing capacity ($CBR \approx 22$) and can thus support the ancient pavement structure. However, both the base and the sub-base layers have lost their initial bearing capacity over time, thus causing a considerable structural defect in the road edifice. Based on the poor behavior of the residual surface layers, it is possible to imagine some best feasible rehabilitation solutions. Nonetheless, it should be noted that in general practice, a road edifice, although properly designed, deteriorates with time at the end of its projected useful life span of 10 - 15 years in Senegal. Hence, to maintain its level of service beyond that period,

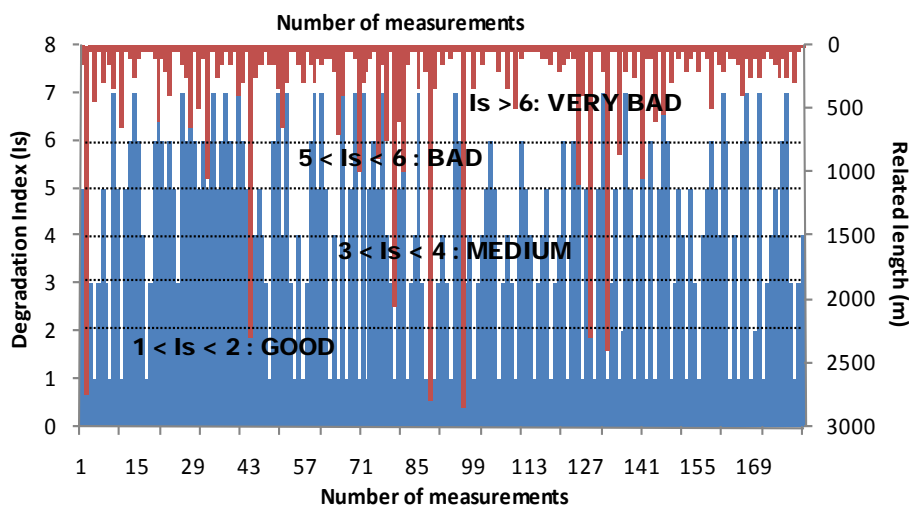


Figure 4. Histogram of the section lengths for surface damages (apparent pavement damages) based on the I_s index [21]. Note: A comparison with Figure 3 suggests a fairly close correspondence between road segments' length with high D_c values and those with high I_s values.

Table 5. Interval of definition for the index (I_s) of surface deterioration on the pavement (VZIR method, [22]).

I_s values	$1 < I_s < 2$	$3 < I_s < 4$	$5 < I_s < 6$	$I_s > 6$
Quality of the pavement	Good	Medium	Bad	Very bad

it must be repaired, usually by constructing a new base layer of cement improved lateritic gravels and capping it with a bituminous pavement cover.

3.4. Summary of the Diagnosis Study

The frequency distribution of the Cd classes, as defined based on **Table 4** and presented in **Figure 5(a)**, revealed that the C1 and C2 class levels are largely dominant, as already shown in **Figure 3**. In addition a cumulative length of approximately 47,686 m (that is about 89.67% of the total length of the road section) has Cd values in the C1 and C2 class levels; thus exhibiting low deflections. This implies a good bearing capacity of the road structure and a relatively good to moderate road quality level. In contrast, a cumulated length of 3,212 m (corresponding to 6.04% of the total length of the road) has Cd values of medium C3 class level which implies a questionable (doubtful) road structure quality level, while a section of 2,279 m (about 4.29% of the road length) exhibited a road structure in the bad quality category (*i.e.* C4 and C5 class levels).

With reference to **Table 7 [3]** which orients the choice of possible solutions in tropical countries according to the profile of Cd values and the apparent surface deteriorations of a road, it can be seen in **Figure 5(b)** that most of the monitored road sections have quality level of the order $\geq Q_3$, which imply a doubtful road quality and the necessity for further investigations.

Table 6. Geotechnical properties of the road layers.

Parameters	PK0 au PK9			PK10 au PK20			PK21 au PK31			PK32 au PK42			PK43 au PK53		
	BL	FL	PF	BL	FL	PF	BL	FL	PF	BL	FL	PF	BL	FL	PF
Grain size fraction < 80 μm (%)	12.30	9.90	9.60	13.10	9.30	10.10	13.80	10.80	10.20	12.30	10.00	9.10	13.50	9.10	10.60
Grain size fraction < 2 mm (%)	29.00	97.10	99.60	29.40	96.90	99.50	31.90	96.80	99.20	32.60	93.80	98.90	30.70	94.30	98.70
Liquidity limit	40.30	-	-	40.80	-	-	32.30	-	-	30.30	-	-	30.70	-	-
Plasticity index	23.00	-	-	22.90	-	-	21.40	-	-	16.40	-	-	16.20	-	-
GTR classification	B6	B2	B2	B6	B2	B2	B6	B2	B2	B6	B2	B2	B6	B2	B2
$\gamma_{d_{\max}}$ (T/m^3)	2.24	1.74	1.73	2.24	1.99	1.69	2.26	1.76	1.77	2.25	1.78	1.78	2.22	1.80	1.79
W OPM (%)	5.20	9.90	10.00	5.00	7.60	10.60	4.40	10.00	9.60	5.00	11.20	11.40	6.60	11.00	11.20
γ_d (95% OPM T/m^3)	2.13	1.65	1.64	2.12	1.89	1.61	2.14	1.67	1.68	2.14	1.69	1.69	2.11	1.71	1.70
CBR index	58.00	17.00	24.00	57.00	18.00	22.00	61.00	19.00	22.00	60.00	18.00	21.00	55.00	19.00	21.00
MBV (g/100g)	-	0.30	0.40	-	0.30	0.40	-	0.30	0.50	-	0.40	0.50	-	0.40	0.50

(Symbols: BL: base layer; FL: fundation layer; PF: plateforme layer).

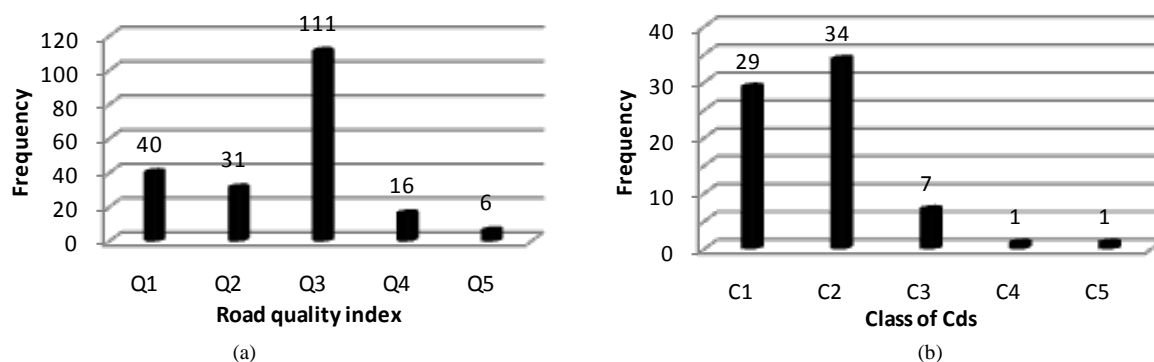


Figure 5. Frequency distribution of the road quality levels (a) and the Cd classes for the monitored road. (Note: The deflection classes C_i are defined in **Table 3**, while the quality indices Q_i are given in **Table 7**).

4. Recommended Rehabilitation Works

Based on the statistics derived from the qualitative ranking (categorization) of the levels of degradation, individual segments' length upon which corrective measures are required were recognized. Such corrective measures take into account the diagnostic results and type of traffic the road was supposed to carry (viz., one equivalent to the T2 traffic type). The recommended solutions to improve the quality of the study road edifice and thus maintain its level of service are: 1) performance of some *maintenance works* on road sections with quality levels of $\leq Q2$; and 2) undertaking of some *reinforcement works* for those sections with quality indices $> Q2$.

Table 8 shows the diagnosis results based on the categorization, and the nature of recommended rehabilitation works according to the recommendations presented in **Table 9** [3]. For comparative purposes, the table also presents the results of the VIZIR study [21] based mainly on the apparent surface conditions of the monitored road (i.e., simply based on the *Is* index of apparent surface deterioration).

Based on the above analyses and discussion, this study recommends:

1) some “*maintenance*” works on road segments with quality levels $< Q3$; that is to say, a rehabilitation of the road pavement by installing a new asphalt layer coating for the degraded zones. The concerned road length is estimated to be about 16.250 km (equivalent to 30.56% of the monitored road section).

2) some “*reinforcement or strengthening*” works on a distance of 36.924 km (nearly some 69.44% of the road length) by providing a new base course of cement treated lateritic gravels (in the usual mixing level of 3% cement) to address the low bearing capacity of the road edifice, and then setting up a bituminous pavement.

However, the VIZIR study [21] finds that 30.650 km of study road (approximately 57.64% of the studied section length) requires some strengthening works, while a length of 22.524 km (~42.36% of the road length) are in suitable condition and would require only minor maintenance works. The discrepancy between the two estimation or evaluation methods is quite substantial; however, the estimates in this study which integrates more index parameters, seems to provide a better understand of the situation of things.

Funding: Further assessment of the cost calculations for the proposed rehabilitation works based on the prevailing market prices revealed a cost estimate in the order of 5,352,000,000 (five billion three hundred fifty-two million) CFA francs, as highlighted in **Table 10**. This cost assessment scenario, which takes into consideration the uncertainties related to the Q3 class level in some of the road sections, is deemed satisfactory based on the dedicated traffic type and desired quality objective.

The funding should be sources from the major financial institutions (e.g., African Bank for Development—ABD and the French Agency for International Development—FAID), which can assist the Senegalese Government in its policy of modernization of the transport infrastructures.

Table 7. Roast decision and parameters taken into account in the development of solutions (modified after [3]).

Road surface appearance	Deflections ($\times 1/100$ m)			
	Low	Cd1= 60	Cd2 = 80	High
Good [<i>Is</i> = 1]	Q1 (maintenance)	Q2 (maintenance)	Q3 (?)	
Cracked but undeformed [<i>Is</i> = 2 - 3]	Q2 (maintenance)	Q3 (?)	Q4 (reinforcement)	
Deformed and cracked [<i>Is</i> = 4 - 7]	Q3 (?)	Q4 (reinforcement)	Q5 (reinforcement)	

Note: The quality scores Q1 and Q2 indicate the need for maintenance works, while note Q3 indicate questionable road quality and requires further analysis for a final appreciation. The higher-order classes (Q4 and Q5) should receive reinforcement works.

Table 8. Results of the diagnosis study for the R31 regional road—quality of the degradations and consistency of recommendation works.

Evaluation criterion	Good	Medium to very bad	Monitored road length
	(Maintenance)	(Reinforcement)	
Quality index (<i>Qi</i>)	16.250 km (30.56%)	36.924 km (69.44%)	53.174 km (100.00%)
Vizir index (<i>Is</i>)	22.524 km (42.36%)	30.680 km (57.64%)	53.204 km (100.00%)

Table 9. Recommendations for the types of repairs according to the road quality index and the traffic class T [3].

Quality level	Traffic type		
	T1	T2	T3
Q1	Regular maintenance		Hatched pattern
Q2	Priority maintenance		
Q3	Reinforcement (10 - 15 cm UTG)		
Q4	Reinforcement (15 - 25 cm UTG)		
Q5	Reinforcement (treated materials)		
>Q5	Hatched pattern		
Surface course refection	New surface coatings by applying a sand-asphalt carpet (2 - 3 cm thick) or a dense BP (4 - 6 cm thick)		

Abbreviations: UTG = untreated gravel; BP = bituminous pavement.

Table 10. Details of the proposed repairs and their cost allocations.

Length of section to be rehabilitated	Current service level	Type of refection	Nature of the work	Unit cost (FCFA/km)	Production cost (FCFA)
16.500 km	Good	Current maintenance	Point in time	8,000,000	132,000,000
5.500 km	Medium	Current maintenance and/or periodic maintenance	Point in time and/or carpet of asphalt (5 cm)	90,000,000	495,000,000
10.000 km	Bad	Periodic maintenance	Base course in lateritic-cement and/or surface layer in asphalt concrete	150,000,000	1,500,000,000
21.500 km	Very bad	Reinforcement	Base course in lateritic-cement and/or surface layer in asphalt concrete	150,000,000	3,225,000,000
Total = 53.500 km				Total = 5,352,000,000	

5. Summary and Conclusions

The structural performance of the R31 regional road was evaluated after more than 10 years of projected service life by means of the Lacroix deflectograph together with other standard methods, while following the French standards and technical specifications used as tools for decision support in road diagnosis and reinforcement.

The study highlights that the main problem lies in a bearing failure of the road structure at some places, following a loss (temporal degradation) of initial properties at the base course and foundation, which show the respective CBR ratios well below the technical specifications. In this particular case, a “reinforcement” aiming at lengthening the service life of the road is recommended, which consists of a layers’ replacement. Elsewhere, where the bearing capacity still remains in good condition, it is recommended that the corrective action should consist of some minor “maintenance”, by introduction of a new pavement coating for the degraded surfaces. A cost saving scenario for such works has been estimated.

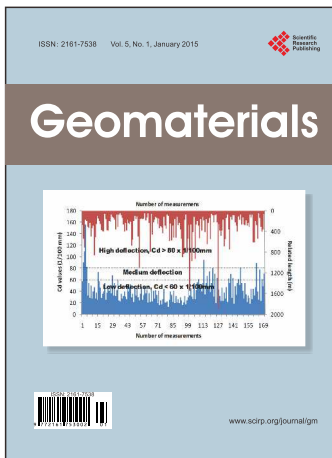
As a form of recommendation, it is essential:

a) to pay a detailed attention to the hydraulic work operations for managing the natural flow and disposal of rain water, by limiting the infiltration on the roadway edges and through carefully executed road shoulders;

b) to carefully study the environment of the road, as well as the hydraulic regime, in order to better understand the origin of the degradations observed on the study road, the rehabilitation of which will allow for revitalization of the agriculture sector which is one of the principal activities in the area.

References

- [1] Norm NF P 94-056 (1995) Grain Size Distribution.
- [2] Norm NF P 11-300 (1992) GTR Sols Classification.
- [3] Norm NF P 94-051 et 052 (1993) Oedometer Methods (Atterberg Limits).
- [4] Norm NF P 94-068 (1998) Methylene Blue Test.
- [5] Norm NF P 94-078 (1997) CBR Test.
- [6] Norm NF P 94-093 (1997) Modified Proctor Test.
- [7] Norm NF P 94-050 (1995) Water Content.
- [8] Centre Experimental de Recherches et d'Etudes du Batiment et des Travaux Publics CEBTP (1980) Guide pratique de dimensionnement des chaussées pour les pays tropicaux. Ministère de la coopération de la république Française, Paris, 155 p.
- [9] Centre Experimental de Recherches et d'Etudes du Batiment et des Travaux Publics CEBTP (1984) Guide pratique de dimensionnement des chaussées pour les pays tropicaux. Ministère des relations extérieures—Coopération et développement de la république Française, Paris, 157 p.
- [10] Centre Experimental de Recherches et d'Etudes du Batiment et des Travaux Publics CEBTP (1985) Manuel pour le renforcement des chaussées souples en pays tropicaux. Ministère de la Coopération de la république française, France, 166 p.
- [11] Laboratoire Central des Ponts et Chaussées LCPC (1997) Etudes routières: Déformabilité de surface des chaussées. Exécution et exploitation des mesures. Méthode d'essai LPC No. 39, Paris, 71 p.
- [12] Centre de Recherches Routières (CRR) (1992) Code de bonne pratique pour le renforcement des chaussées souples à l'aide de matériaux bitumineux. CRR R56/85, Groupe de travail Dimensionnement des chaussées, D/1992/0690/1, Bruxelles, 75 p.
- [13] Centre d'Etudes sur les Réseaux, les Transports, l'Urbanisme et les Constructions CERTU (2005) Matériels et méthodes d'auscultation des chaussées urbaines, hors collection. CERTU 2005/6, Lyon, 66 p.
- [14] Wukler, S. (2010) Développement de techniques d'auscultation de chaussées. Projet de Fin d'Etudes, INSA de Strasbourg, Génie Civil Option ATE, 63 p. http://eprints2.insa-strasbourg.fr/634/1/Rapport_PFE.pdf
- [15] Nkembo, P.M.E. (2013) Mesures des deflections d'une chaussee avec le deflectographe Lacroix: Cas de route regionale R31 Louga-Ouarack-Ndoyene. Memoire IST No. 274, Faculte des Sciences et Techniques, universite Cheikh Anta Diop de Dakar, Dakar, 50 p.
- [16] Millien, A., Petit, C. and Takarli, M. (2009) Rapport diagnostic de chaussée du CD36. Convention entre la Plateforme Travaux Public du Limousin et le Conseil de la Corrèze, Université de Limoges, 14 p. <http://www.pft-travauxpublics-limousin.com/files/annexe6.pdf>
- [17] Henia, M.O. and Braber, R. (2008) Falling Weight Deflectometer et Défectographe Lacroix: Comparaison, Domaine d'Application et Perspectives. Suisse, 6 p. <http://www.infralab.ch/wp-content/uploads/2013/12/Article-RT-Comparaison-HWD-et-Lacroix.pdf>
- [18] Association Française de Normalisation AFNOR (1991) Norme NF P 98-200-1—Essais relatifs aux chaussées. Mesure de la déflexion engendrée par une charge roulante. Partie 1: Définitions, moyens de mesure, valeurs caractéristiques. 1991/7, Paris, 6 p.
- [19] Association Française de Normalisation AFNOR (1993) Norme NF P 98-200-3—Essais relatifs aux chaussées. Mesure de la déflexion engendrée par une charge roulante. Partie 3: Détermination de la déflexion avec le défectographe 02. 1993/9, Paris, 6 p.
- [20] Andrén, P. (2006) Development and Results of the Swedish Road Deflection Tester. Licentiate Thesis from Royal Institute of Technology Department of Mechanics, Stockholm, 95 p. <http://www.diva-portal.org/smash/get/diva2:10556/FULLTEXT01.pdf>
http://www.peterandren.se/licrep/licrep_eng.php#x1-90001.4
- [21] APAVE Sahel (2012) Organisation et exécution d'une campagne d'inspections sommaires sur le réseau routier classé (Routes revêtues de toutes les régions du Sénégal). Rapport Interne, Dakar, 88 p.
- [22] Laboratoire Central des Ponts et Chaussées (1991) VIZIR: Méthode assistée par ordinateur pour l'estimation des besoins en entretien d'un réseau routier. LPCP, Paris, 63 p.



Call for Papers

Geomaterials (GM)

ISSN 2161-7538 (Print) ISSN 2161-7546 (Online)

<http://www.scirp.org/journal/gm>

Geomaterials (GM) is open to original research articles accepting rock and soil as material. In addition to original research applications review papers and short technical notes are accepted. Geomaterials forms a platform to publish articles from experimental researches, theoretical analysis, statistical and mathematical modeling work. In addition, papers condensed on the analysis, modeling and optimization efforts in industry scale projects or applications are accepted.

Subject Coverage

This journal invites original research and review papers that address the following issues. Topics of interest include, but are not limited to:

- 3d modelling of ore bodies.
- Blasting performance: Rock response to blasting, fragmentation quality, seismic loading, and effects of rock structural elements in wave transmission.
- Characterization of geomaterials: Experimental methods in determining physical and mechanical parameters of geomaterials.
- Dampening and permeability properties: Seismic wave dampening characteristics, fluid, gas and radiation flow or emitting behavior of geomaterials.
- Geostatistics.
- Mine mechanization.
- Mining/extraction of geomaterials/minerals.
- Modeling the behavior of geomaterials: results of the efforts behavior or response of geomaterials using statistical, mathematical and numerical methods.
- Monitoring behavior: Methods and equipment to monitor behavior of geomaterials.
- Results of the experimental and industrial applications: Applications focused on behavior of geomaterials.
- Size reduction: Characteristics and response to grinding effects, mechanism of processes.
- Soil behavior: Characteristics and response of soil related with the engineering processes.
- Wear and cutting behavior of geomaterials: The mechanism in drilling, cutting and sawing processes need extended work to explain the response of geomaterials to mechanical effect. Drilling, mechanical excavation, sawing and abrasive water jet machining are in the primary concern in that sense.

We are also interested in short papers (letters) that clearly address a specific problem, and short survey or position papers that sketch the results or problems on a specific topic. Authors of selected short papers would be invited to write a regular paper on the same topic for future issues of the GM.

Notes for Intending Authors

Submitted papers should not have been previously published nor be currently under consideration for publication elsewhere. Paper submission will be handled electronically through the website. All papers are refereed through a peer review process. For more details about the submissions, please access the website.

Website and E-Mail

<http://www.scirp.org/journal/gm>

E-mail: gm@scirp.org

What is SCIRP?

Scientific Research Publishing (SCIRP) is one of the largest Open Access journal publishers. It is currently publishing more than 200 open access, online, peer-reviewed journals covering a wide range of academic disciplines. SCIRP serves the worldwide academic communities and contributes to the progress and application of science with its publication.

What is Open Access?

All original research papers published by SCIRP are made freely and permanently accessible online immediately upon publication. To be able to provide open access journals, SCIRP defrays operation costs from authors and subscription charges only for its printed version. Open access publishing allows an immediate, worldwide, barrier-free, open access to the full text of research papers, which is in the best interests of the scientific community.

- High visibility for maximum global exposure with open access publishing model
- Rigorous peer review of research papers
- Prompt faster publication with less cost
- Guaranteed targeted, multidisciplinary audience



**Scientific
Research
Publishing**

Website: <http://www.scirp.org>

Subscription: sub@scirp.org

Advertisement: service@scirp.org